AD NUMBER
ADA801178
CLASSIFICATION CHANGES
TO: **unclassified**
FROM: **restricted**
LIMITATION CHANGES
TO: **Approved for public release; distribution is unlimited.**
FROM: **Distribution authorized to DoD only; Administrative/Operational Use; 11 MAY 1950. Other requests shall be referred to National Aeronautics and Space Administration, Washington, DC. Pre-dates formal DoD distribution statements. Treat as DoD only.**
AUTHORITY
NACA Res. Abstracts no. 46 dtd 3 Jul 1953; NASA TR Server website

Reproduction Quality Notice

This document is part of the Air Technical Index [ATI] collection. The ATI collection is over 50 years old and was imaged from roll film. The collection has deteriorated over time and is in poor condition. DTIC has reproduced the best available copy utilizing the most current imaging technology. ATI documents that are partially legible have been included in the DTIC collection due to their historical value.

If you are dissatisfied with this document, please feel free to contact our Directorate of User Services at [703] 767-9066/9068 or DSN 427-9066/9068.

Do Not Return This Document To DTIC

REEL-C 3556B

A.T.I 75592

BY Arthur E. Creech

RESTRICTED

ERRATA

NACA RM L50C02a

HIGH-SUBSONIC PERFORMANCE CHARACTERISTICS AND BOUNDARY-LAYER INVESTIGATIONS OF A 12° 10-INCH-INLET-DIAMETER CONICAL DIFFUSER

By B. H. Little, Jr. and Stafford W. Wilbur

May 11, 1950

Page 7, lines 1 and 2: Revise the sentence as follows: The parameter p_{ref}/H_o is plotted against local Mach number and mean inlet Reynolds number in figure 6.

Page 24, figure 6: Change vertical scale labels to read "Mean inlet Reynolds number $\times 10^{-6}$" and "Local Mach number." Change title below figure to "Variation of local Mach number and mean inlet Reynolds number with the correlating pressure ratio p_{ref}/H_o."

NACA-Langley - 4-27-51 - 400

RESTRICTED

Copy
RM L50C02a

NACA

RESEARCH MEMORANDUM

HIGH-SUBSONIC PERFORMANCE CHARACTERISTICS AND BOUNDARY-LAYER INVESTIGATIONS OF A 12° 10-INCH-INLET-DIAMETER CONICAL DIFFUSER

By B. H. Little, Jr. and Stafford W. Wilbur

Langley Aeronautical Laboratory
Langley Air Force Base, Va.

NATIONAL ADVISORY COMMITTEE
FOR AERONAUTICS

WASHINGTON

May 11, 1950

NATIONAL ADVISORY COMMITTEE FOR AERONAUTICS

RESEARCH MEMORANDUM

HIGH-SUBSONIC PERFORMANCE CHARACTERISTICS AND BOUNDARY-LAYER INVESTIGATIONS OF A 12° 10-INCH-INLET-DIAMETER CONICAL DIFFUSER

By B. H. Little, Jr. and Stafford W. Wilbur

SUMMARY

Performance and boundary-layer data were taken in a 12° 10-inch-inlet-diameter conical diffuser of 2:1 exit- to inlet-area ratio. These data were taken for two inlet-boundary-layer conditions. The first condition was that of a thinner inlet boundary layer (boundary-layer displacement thickness, $\delta^* \approx 0.034$) produced by an inlet section approximately 1 inlet diameter in length between the entrance bell and the diffuser. The second condition was a thicker inlet boundary layer ($\delta^* \approx 0.120$) produced by an additional inlet section length of approximately 6 diameters.

Longitudinal static-pressure distributions were measured from wall static orifices. Transverse total- and static-pressure surveys were made at the inlet and exit stations. Boundary-layer velocity distributions were measured at seven stations between the inlet and exit. These data were obtained for a Reynolds number (based on inlet diameter) range of 1×10^6 to 3.9×10^6. The corresponding Mach number range was from $M = 0.2$ to choking. At the maximum-power-available condition supersonic flow was obtained as far as 4.5 inches downstream from the diffuser inlet with a maximum Mach number of $M \approx 1.5$.

The total-pressure loss through the diffuser in percentage of inlet dynamic pressure was approximately 2.5 percent for the thinner inlet boundary layer and 5.5 percent for the thicker inlet boundary layer over the lower subsonic range. These values increased with increasing flow rate — the values for the thicker inlet boundary layer more than those for the thinner inlet boundary layer. The diffuser effectiveness, expressed as the ratio of the actual static-pressure rise to the ideal static-pressure rise, was about 85 percent for the thinner inlet boundary

layer and about 67 percent for the thicker inlet boundary layer in the lower subsonic range. These values decrease with increasing flow rate.

Separated flow was observed for both inlet-boundary-layer conditions in the region of adverse pressure gradient just downstream of the transition curvature from inlet section to diffuser. The flow for the thinner-inlet-boundary-layer condition did not fully re-establish itself along the diffuser walls. The thicker inlet-boundary-layer flow, while not completely re-establishing the normal flow pattern downstream of the separated region, did re-establish more successfully than the thinner inlet boundary layer.

INTRODUCTION

The design of diffusers to meet the specifications of jet power plants operating at high-subsonic Mach numbers and correspondingly high Reynolds numbers is hindered somewhat by a lack of knowledge of the relation of boundary-layer growth to performance characteristics. Although much has been done in the study of diffuser performance and boundary-layer action in diffusers, the applicability of this work to present-day aircraft is limited somewhat because most of the investigations were made at low Mach numbers and/or Reynolds numbers.

For example, Gibson's (reference 1) classic experiments in 1909 determining pressure losses of water flow in conical diffusers ranged only up to Reynolds numbers of approximately 2×10^3 at velocities up to 23 feet per second, and no attempt was made to control inlet boundary layer. Squire (reference 2) investigated diffuser performance using a constant-inlet-length configuration at a Reynolds number of 1×10^6 and Mach number of approximately 0.4. Straight-walled conical diffusers with inner bodies and with negligible inlet-boundary-layer thickness were investigated by Bohm and Koppe (reference 3) for Mach numbers up to choking and Reynolds numbers up to 1.4×10^5. Naumann (reference 4) studied low-angle conical diffusers with inlet lengths of 1.2 diameters for Mach numbers up to choking and Reynolds numbers up to 2×10^6. Peters (reference 5) who studied the effects of varying the inlet boundary layer and the diffusion angle, reached a maximum Reynolds number of 2×10^5 at a Mach number of approximately 0.12. The inlet boundary layer was varied by adding straight pipe 6 to 64 inlet diameters long to the diffuser entrance. References 6 and 7 summarize a large portion of the earlier available data on diffuser performance.

The purpose of the present investigation is to study the influence of inlet-boundary-layer conditions upon boundary-layer action in the

diffuser and the consequent influence upon diffuser performance at inlet Reynolds and Mach numbers characteristic of those encountered in flight.

The data presented herein were obtained from investigations conducted in the Langley internal aerodynamics laboratory. A 12° 10-inch-inlet-diameter conical diffuser with exit- to inlet-area ratio of 2:1 and followed by a 28-inch-long tailpipe was used. Inlet Mach number was varied from 0.2 to choking and inlet-diameter-based Reynolds number from 1×10^6 to 3.9×10^6. Inlet-boundary-layer conditions were varied by using two different lengths of inlet pipe, one 9 inches long and the other 68 inches long. This report represents the third part of an investigation of three diffuser configurations with 2:1 area ratio and varying inlet-boundary-layer conditions. Reference 8 reports the investigation of a 12° 21-inch-inlet-diameter diffuser, and reference 9, a 23° 21-inch-inlet-diameter diffuser.

SYMBOLS

p	static pressure
H	total pressure
ΔH	total-pressure loss
Δp	static-pressure rise
q	compressible impact pressure $(H - p)$
Δq	change in impact pressure
u	local velocity within boundary layer
U	local velocity at edge of boundary layer
x	longitudinal distance along diffuser
y	perpendicular distance from diffuser wall
δ	boundary-layer thickness at $0.95u/U$, inches
δ'	boundary-layer thickness at $1.00u/U$, inches
δ^*	boundary-layer displacement thickness, inches $\left(\int_0^{\delta'} \left(1 - \frac{u}{U}\right) dy\right)$

θ	boundary-layer momentum thickness, inches $\left(\int_0^{\delta'} \frac{u}{U}\left(1-\frac{u}{U}\right)dy\right)$
δ^*/θ	boundary-layer-shape parameter
$\Delta H/q_1$	loss coefficient
$\Delta p/\Delta q$	pressure efficiency
$\Delta q/\Delta q_{ideal}$	diffusion factor
$\Delta p/\Delta p_{ideal}$	diffuser effectiveness

Subscripts:

o	reference stagnation conditions
i	diffuser inlet conditions
e	diffuser exit conditions

Boundary-layer stations numbered from 1 to 7.

APPARATUS

The apparatus, as shown in the line diagram of figure 1, consists of the entrance bell, the variable-length, constant-diameter inlet section, the conical diffuser, and the tailpipe or exit section. The diffuser itself is constructed in two parts. The first part consists of an inlet length of 9 inches leading to the diffuser, a transition region between the straight inlet and the conical diffuser section, and the first 9 inches of the diffuser. The other part is a truncated cone section 10.6 inches long which completes the diffuser. The diffuser has a 10-inch-diameter inlet and 14.1-inch-diameter exit to give an exit-to inlet-area ratio of 2:1. The included conical angle is 12°.

All sections were formed from $\frac{1}{2}$-inch cold-rolled steel and all inner surfaces except those of the tailpipe were machined, painted, and then finished with No. 600 wet or dry sandpaper. All joints were sealed with pyroxylin and sanded smooth.

For the thinner-inlet-boundary-layer condition, only the 9 inches of inlet pipe integral with the diffuser was used. For the thicker inlet boundary layer, a 59-inch inlet section was added to make a total of 68 inches. The short inlet configuration is shown in figure 2 and the long inlet configuration in figure 3.

Static-pressure orifices were installed along a generatrix of the conical diffuser and in the inlet pipe at convenient increments of distance. Six additional static-pressure orifices were equally spaced circumferentially at the inlet and exit stations of the diffuser. In the transition region, six static-pressure orifices were very closely spaced (see inset, fig. 1) in order to measure accurately the pressure changes through this region. Since these orifices were located at such small longitudinal increments of distance, it was necessary to stagger them circumferentially over a distance of about $1\frac{1}{2}$ inches.

Air was supplied by two centrifugal blowers in series which could deliver 22,000 cubic feet per minute at approximately 1.4 atmospheres to the diffuser entrance bell. In order to obtain temperatures high enough to avoid condensation, air was recirculated in a semiclosed circuit system.

Stagnation temperature and pressure measurements were made upstream of the entrance bell. Temperature was measured with an iron-constantan thermocouple and potentiometer pyrometer, and total pressure was measured with a shielded total-pressure tube. All pressure measurements were made with multitube manometers containing tetrabromoethane.

Boundary-layer total-pressure measurements were made with the rake shown in figure 4. The tubes varied in size from 0.030-inch outside diameter at the wall to 0.050-inch outside diameter farther out. A static-pressure tube was mounted on the rake to measure static pressures at the same longitudinal station as the total pressures were measured. In some cases, near the diffuser exit the boundary layer was so thick that the rake did not entirely cover the distance δ and supplementary measurements were made with a movable pitot-static tube. This movable pitot-static tube was designed to survey total and static pressures across the inlet and exit stations. As shown in figure 5, it was telescoped from $\frac{1}{8}$-inch outside diameter at the upstream end to $\frac{5}{8}$-inch outside diameter at the downstream end. In the tailpipe it was rigidly attached to a streamline tube strut which could be moved transversely to survey from wall to wall. By substituting tubes of various lengths it was possible to survey pressures at any station in the diffuser.

Although the movable pitot-static tube used to obtain velocity values to supplement those read by the boundary-layer rake was always directed parallel to the diffuser axis, such errors as would be introduced by the inclination of the flow to the tube at any point in the diffuser are negligible. The maximum inclination would probably be less than 6°, and in reference 10 it is shown that for a similar pitot-static tube the error in measured velocity at such angles of flow inclination is less than 1 percent.

COMPUTATIONAL METHODS

The ratio of the velocity inside the boundary layer to the velocity at the edge of the boundary layer was determined by the following formula:

$$\frac{u}{U} = \sqrt{\frac{H_x - p_x}{H_{max} - p_x}}$$

It was found that the error in values of H caused by using this incompressible formula was less than -5 percent up to local Mach numbers of about 0.7. Beyond this point the error increased gradually up to about -20 percent at local $M = 1.0$. Since most of the data presented are in the range where the local $M < 0.7$, the simplified incompressible equation was used throughout.

Only incompressible values of the parameters δ^*, θ, and δ^*/θ are presented. It was found that these values are adequate for comparison of profile shapes under the conditions of this investigation. Also, since much of the available data are presented in the incompressible form, comparison with these data is made easier.

The graphical integration used to obtain δ^* and θ from velocity profiles did not include the area bounded by the reversed-flow portion of the separated-flow profile and the u/U axis because the instrumentation used was not able to measure negative velocities. Therefore the values of δ^* and θ for the separated profiles will be in error by some negative amount, depending upon the severity of the separation.

The ratio of the inlet reference static pressure to the stagnation pressure p_{ref}/H_o is used as a correlating parameter for the performance and boundary-layer curves. Decreasing values of p_{ref}/H_o indicate increasing rate of flow. The position of the orifice used for p_{ref} is

shown in figure 1. The parameter p_{ref}/H_o is plotted against mean inlet Mach number and inlet Reynolds number in figure 6.

The total-pressure losses through the diffuser were determined from weighted averages of pressure surveys at the inlet and exit by the method explained in reference 9:

$$\frac{\Delta H}{H_o} = \frac{\overline{H_o - H_e}}{H_o} - \frac{\overline{H_o - H_i}}{H_o}$$

The change of impact pressure then could be obtained from the equation:

$$\frac{\Delta q}{H_o} = \frac{\Delta H}{H_o} - \frac{\Delta p}{H_o}$$

DISCUSSION

Performance

Four parameters are used to present the performance data. These are the loss coefficient $\Delta H/q_i$, the pressure efficiency $\Delta p/\Delta q$, the diffusion factor $\Delta q/\Delta q_{ideal}$, and the diffuser effectiveness $\Delta p/\Delta q_{ideal}$.

The ratio $\Delta H/q_i$ is a convenient measure of pressure loss because it possesses the tendency to remain constant with varying density and flow rate as long as the flow pattern does not change.

The pressure efficiency and diffusion factor are measures of different components of diffuser effectiveness, and each is useful in analyzing diffuser performance.

The pressure efficiency $\Delta p/\Delta q$ measures how much of the impact-pressure drop through the diffuser is converted to static pressure and depends upon friction and shock losses.

The diffusion factor $\Delta q/\Delta q_{ideal}$ measures how much of the geometric expansion is utilized to convert impact pressure to static pressure. Anything, such as thickening boundary layer, which reduces the effective expansion ratio will reduce $\Delta q/\Delta q_{ideal}$.

An over-all measure of the ability of a diffuser to convert the entering impact pressure to static pressure at the exit is the ratio $\Delta p_{actual}/\Delta p_{ideal}$ which is the product of the pressure efficiency and diffusion factor, since

$$\Delta q_{ideal} = \Delta p_{ideal}$$

$$\frac{\Delta p_{actual}}{\Delta p_{ideal}} = \frac{\Delta p}{\Delta q} \frac{\Delta q}{\Delta q_{ideal}}$$

This ratio is called diffuser effectiveness.

Loss coefficient.- The loss coefficient $\Delta H/q_1$ is plotted against p_{ref}/H_o for both the thinner and thicker inlet boundary layers in figure 7. For the thinner inlet boundary layer $\Delta H/q_1$ is practically constant at 0.025 through most of the subsonic range. The value increases slightly in the high-subsonic range and increases sharply when supersonic flow, with subsequent shock losses, is obtained. For the thicker-inlet-boundary-layer condition $\frac{\Delta H}{q_1} = 0.055$ through the low-subsonic range. In the range above $M = 0.7$ $\left(\text{that is, } \frac{p_{ref}}{H_o} \approx 0.7\right)$, $\frac{\Delta H}{q_1}$ increases much more rapidly with increasing flow rate than was the case for the thinner inlet boundary layer. At flow rates where supersonic flow was attained, the curve breaks upward rapidly as in the case of the thinner inlet boundary layer.

Diffusion factor.- The diffusion factor is plotted in figure 8. In the low-subsonic-flow range, for the thinner inlet boundary layer $\frac{\Delta q}{\Delta q_{ideal}} \approx 0.86$, and for the thicker inlet boundary layer $\frac{\Delta q}{\Delta q_{ideal}} \approx 0.73$. Comparison with the values of $\Delta q/\Delta q_{ideal}$ in reference 8 shows that for each condition the values for this 10-inch-diameter diffuser are about 0.10 lower than for the 21-inch-diameter diffuser of that reference. Further comparison, however, leads to an explanation of this, for in each inlet-boundary-layer condition, the values of $\left(\frac{\delta^*}{\text{Diameter}}\right)_1$ are higher for the smaller diffuser.

Pressure efficiency.– The pressure efficiency $\Delta p/\Delta q$ is plotted in figure 9. This parameter, since it measures the ability of the diffuser to convert the change in impact pressure through the diffuser to static pressure, will be largely dependent upon pressure losses through the system and therefore can be expected to vary similarly to $\Delta H/q_1$. It is seen therefore that for the thin-inlet-boundary-layer condition $\Delta p/\Delta q$ is practically constant at approximately 0.96 until shock losses cause a sharp downward trend when the system chokes. For the thicker inlet boundary layer $\Delta p/\Delta q$ is fairly constant over the lower subsonic range at about 0.90 but in the higher subsonic flow range the values drop off much more rapidly with increasing flow rate than the thinner-inlet-boundary-layer curve.

Diffuser effectiveness.– The diffuser effectiveness $\left(\frac{\Delta p}{\Delta p_{ideal}} = \frac{\Delta q}{\Delta q_{ideal}} \frac{\Delta p}{\Delta q}\right)$ is plotted against p_{ref}/H_o in figure 10. For the thinner inlet boundary layer $\frac{\Delta p}{\Delta p_{ideal}}$ is constant at about 0.825 in the lower subsonic flow range and decreases slowly with increasing flow rate until choking condition is reached, at which point the values drop rapidly. For the thicker inlet boundary layer $\frac{\Delta p}{\Delta p_{ideal}} \approx 0.67$ at low flow rates and the curve behaves in a manner similar to that of the thinner inlet boundary layer.

In the unchoked condition the performance of the thinner-inlet-boundary-layer configuration appears to be better in every respect. The effectiveness of the thicker-inlet-boundary-layer configuration appears to have been affected more by the decrease in effective expansion ratio $\left(\text{as represented by the decrease in } \Delta q/\Delta q_{ideal}\right)$ than by the increase in pressure losses in the thicker boundary layer (as represented by $\Delta p/\Delta q$).

STATIC-PRESSURE DISTRIBUTION

In reference 11 it is pointed out that one of the variables that control the development of turbulent boundary layer is the existing pressure gradient. A good visualization of the pressure gradients existing in the two diffuser configurations can be obtained from the plots of the ratio of absolute static pressure measured along the wall to the reference total pressure p/H_o for the thinner inlet boundary layer in figure 11 and for the thicker inlet boundary layer in figure 12.

The point $x = 0$ in these figures and all subsequent discussion is the point where the inlet pipe is tangent to the transition region curvature.

Certain general characteristics of these static-pressure-distribution curves are common to both thinner- and thicker-inlet-boundary-layer cases. For both there exists a favorable pressure gradient through the converging entrance bell, the inlet pipe that is effectively converging due to boundary-layer growth, and into the diffuser transition region where local acceleration is created. It is of interest to note that for both the thinner- and thicker-boundary-layer cases at all subcritical flow rates the point of minimum static pressure is located at $x = 0.60$ which is about 0.10 inch downstream of the point where the transition curvature ends.

At the subcritical flow rates a strong adverse gradient begins at about $x = 0.6$ inch for both cases. The adverse gradient is maintained throughout the diffuser but the intensity decreases with increasing distance downstream.

At supercritical flow rates the flow expands supersonically in the diverging passage and the favorable pressure gradient is extended until terminated by shock waves. These shock waves produce strong nonisentropic compressions which restore the flow to subsonic state with strong adverse pressure gradients as in the subcritical inlet-velocity case.

A comparison of the relative strengths and positions of the pressure gradients is presented in figure 13 where p/H_o curves corresponding to the same values of p_{ref}/H_o are plotted for the thinner- and thicker-inlet-boundary-layer conditions.

To obtain the curves of figure 13 at the same values of p_{ref}/H_o for each inlet-boundary-layer condition, the following procedure was used.

In the unchoked condition, a cross plot of figure 12 was obtained by plotting static pressure at each orifice against p_{ref}/H_o. Then for any value of p_{ref}/H_o for which a pressure-distribution curve was available for the thinner-inlet-boundary-layer condition, a faired curve could be obtained for the thicker-inlet-boundary-layer condition. When the diffuser choked, however, a situation arose which made it impossible to continue this method of comparison. The thicker inlet boundary layer was affected by the negative pressure gradient existing in the transition region farther upstream than the thinner inlet boundary layer. For the thicker-inlet-boundary-layer case a thinning of the boundary layer

occurred farther upstream in the inlet section. This process did two things: (1) It created an effective throat upstream of that found in the thinner-inlet-boundary-layer case, and (2) it increased the effective radius of curvature in the transition region. If the point where $\frac{p}{H_o} = 0.528$ $(M = 1.0)$ is considered to be the effective throat it can be seen in figure 13 that for the thicker-inlet-boundary-layer case the throat is displaced approximately 2 inches upstream of that for the thinner-inlet-boundary-layer case and approximately 3 inches upstream of the point where the transition region begins. Therefore, when the system was choked, the thicker-inlet-boundary-layer case attained values of p_{ref}/H_o as low as 0.528, whereas the thinner-inlet-boundary-layer case could not attain values lower than $\frac{p_{ref}}{H_o} = 0.56$. This made it impossible to compare static-pressure-distribution curves from the two cases with equal values of p_{ref}/H_o for the choked condition. Therefore, two arbitrary curves were selected from each case - one being the first choked point obtained, and the second being at the maximum-power-available condition.

In figure 13 it can be seen that the pressure gradients throughout the diffuser are not as great for the thicker inlet boundary layer as for the thinner inlet boundary layer. In the transition curvature region this is caused by the difference in effective radii of curvature created by the cushioning effect of the thicker boundary layer, and in the diffuser by the decreasing of effective expansion area created by the thicker boundary layer.

Radial distributions of static pressure, plotted as the ratio of absolute static pressure to reference stagnation pressure, at the inlet and exit stations are shown for the thinner inlet boundary layer in figure 14 and for the thicker inlet boundary layer in figure 15. Some radial surveys of static pressure (not shown) were also made at stations 5 and 6 for the thicker inlet boundary layer. At subcritical velocities the maximum variation of local static pressure from the value at midstream was less than ±3 percent. The first profiles to show a variation greater than 3 percent occurred at $\frac{p_{ref}}{H_o} \approx 0.57$. At the highest flow rates, however, variations as great as 30 percent were found.

It was also found that reference stagnation pressure existed at the diffuser center line in all cases except where shock losses occurred. For the subcritical flow rates, therefore, the values plotted of p/H_o in figures 11 and 12 can be taken as the local midstream values of p/H and the local Mach number obtained accordingly.

Boundary Layer

Thinner inlet boundary layer.- Representative boundary-layer velocity profiles at each survey station are plotted for the thinner inlet boundary layer in figures 16(a) to 16(g). The boundary-layer thickness, δ, is plotted against p_{ref}/H_o in figure 17; δ^* is plotted against p_{ref}/H_o in figure 18 and against x in figure 19; θ is plotted against p_{ref}/H_o in figure 20 and against x in figure 21; and δ^*/θ is plotted against p_{ref}/H_o in figure 22 and against x in figure 23.

In some cases certain deficiencies in the data exist which require some explanation prior to an analysis of these figures. Near the diffuser exit (see fig. 16(f)) the data taken were incomplete in that the boundary-layer thickness was greater than the 2-inch span of the boundary-layer survey rake. In these cases it was believed that the velocity distributions within the rake's span were of enough significance to present the data using H_o as the value of total pressure at the edge of the boundary layer. When this was done, solid lines were used to connect only the actual data points, and broken lines were used to represent the fairing of the profile to the midstream velocity as computed from the H_o values.

At the high flow rates where supersonic flow existed near the diffuser inlet, total-pressure surveys downstream of this region showed a deficiency from the reference value which was caused by shock losses. An extreme example of this is shown for $\frac{p_{ref}}{H_o} = 0.561$ in figure 16(g). In these cases it is impossible to determine at what point the boundary-layer pressure loss ends, so U was computed at the point where the maximum total pressure was measured. No attempt was made to determine δ^* or θ except in those cases where the maximum total pressure was equal to H_o.

For the separated profiles (in the present discussion, a separated profile is arbitrarily defined as one in which the point $\frac{u}{U} = 0$ is displaced a measurable distance from the wall) some significance of the boundary-layer parameters is lost, particularly in the case of δ^*/θ, for the single-parameter representation (reference 11) is no longer applicable. These parameters do retain some value, however, for comparative purposes and therefore are presented. All points on the boundary-layer curves that were obtained from separated profiles are indicated in each figure. No attempt is made to fair curves through these points. They are connected with dotted lines and are presented merely to show the points at which separation was observed.

At subsonic inlet velocities where $\frac{p_{ref}}{H_o} > 0.65$, the flow pattern appears as a well-established flow except near the diffuser exit. At station 5 one separated profile was observed at the lowest flow rates. At stations 6 and 7, however, the flow pattern is very unstable and appears to follow no definite trends throughout the flow range. When the inlet velocity approached the point where local sonic velocity is attained in the transition curvature, separated profiles were observed at station 3, but the flow was reattached at station 5. When supersonic velocities were attained, all the profiles downstream of the shock terminating the supersonic region were separated.

As shown in figure 17, δ remains practically invariant at stations 1 and 2 with increasing velocity. In the diffuser itself, however, δ varies directly as a function of distance downstream from the inlet and inlet velocity. Figures 18, 19, 20, and 21 show that δ^* and θ vary in a manner similar to that of δ.

From the plots of figure 20 it appears that it is impossible to fix a value of δ^*/θ where separation will occur. In agreement with the findings of reference 11, however, separated profiles were not observed at $\frac{\delta^*}{\theta} < 1.8$ nor attached profiles at $\frac{\delta^*}{\theta} > 2.6$ except for one or two isolated cases. Figure 23 provides a good picture of the regions in the diffuser where separation troubles occur for any flow rate. In general, at low flow rates, separation trouble begins near the diffuser exit, and at high flow rates near the diffuser inlet.

Thicker inlet boundary layer.- Boundary-layer profiles at station 1 for the thinner- and the thicker-inlet-boundary-layer conditions are plotted nondimensionally in figure 24. This plot offers a good comparison of the two inlet-boundary-layer conditions. This comparison shows that, in the case of the thicker inlet boundary layer, higher velocity air from midstream has mixed with the lower velocity air near the wall more completely than for the thinner inlet boundary layer. Thus it appears that the thicker-inlet-boundary-layer flow should offer more resistance to separation than the thinner-inlet-boundary-layer flow. This observation is borne out by data which will be discussed later.

Boundary-layer profiles in the diffuser are plotted for the thicker-inlet-boundary-layer condition in figure 25. At the extreme low flow rates, separation occurred at stations 5, 6, and 7. Through most of the subsonic-flow range, however, the flow remained attached throughout the diffuser. At station 3 at $\frac{p_{ref}}{H_o} < 0.65$, a small region of separated

flow was observed. The flow was reattached at station 4. At supercritical velocities, shock-produced separation occurred as in the case of the thinner inlet boundary layer.

Boundary-layer thickness δ is plotted against p_{ref}/H_o in figure 26. At stations 1 and 2, in the region of favorable pressure gradient, δ decreases with increasing flow rate but in the diffuser δ increases with increasing flow rate and distance from the inlet. The plots of δ^* against p_{ref}/H_o in figure 27, δ^* against x in figure 28, θ against p_{ref}/H_o in figure 29, and θ against x in figure 30 show about the same type variation as δ except at the lowest flow rates where the separated flow occurs. It is of interest to note the correlation between δ^* (fig. 27) and the performance parameter $\Delta q/\Delta q_{ideal}$ (fig. 8). For the thicker inlet boundary layer it can be seen that when δ^* is high and the effective area of the diffuser is reduced at the lowest flow rates, $\Delta q/\Delta q_{ideal}$ is also reduced below the peak value. The minimum values of δ^* at $\frac{p_{ref}}{H_o} \approx 0.92$ are accompanied by the maximum value of $\Delta q/\Delta q_{ideal}$. Similar correlation can be observed for the thinner-inlet-boundary-layer condition (fig. 18).

Figures 31 and 32, in which the shape factor δ^*/θ is plotted against p_{ref}/H_o and x, respectively, show that the thicker inlet boundary layer is more stable than the thinner inlet boundary layer (see fig. 23) except at the lowest flow rates. At high-subsonic flow rates $\frac{p_{ref}}{H_o} \leq 0.7$ there is the same region of separated flow at station 3 that was observed for the thinner inlet boundary layer, but the flow appears to have re-established its normal pattern at station 5.

There are two regions in the plot of δ^*/θ against x where the thicker-inlet-boundary-layer flow appears notably different from the thinner-inlet-boundary-layer flow. At station 3 there is no sharp increase in values of δ^*/θ at the high flow rates (fig. 32) as there was for the thinner-inlet-boundary-layer flow (fig. 23). This is due to two things: (1) the thicker-inlet-boundary-layer profile appears more fully developed at the entrance of the diffuser (fig. 24); and (2) the adverse pressure gradients in the region just downstream of the transition curvature are not as severe for the thicker inlet boundary layer as for the thinner inlet boundary layer. At station 6, where at the low flow rates for the thinner inlet boundary layer there were high values of δ^*/θ, the variation of δ^*/θ with x for the thicker inlet

boundary layer is comparatively steady. It appoars that the transfer of energy from the central flow core into tho boundary layer is moro nearly sufficient to maintain flow in the thicker inlet boundary layer than in the case of the thinner inlet boundary layer at these flow rates.

CONCLUSIONS

For the two inlet-boundary-layer thicknesses (boundary-layer displacement thickness, $\delta^* \approx 0.034$ and $\delta^* \approx 0.120$) investigatod in a 12° 10-inch-inlet-diameter conical diffuser of 2:1 area ratio, the following conclusions are drawn:

(1) For the thinner inlet boundary layer the total-pressuro loss is practically constant with varying flow rate at 2.5 percent of inlet dynamic pressure through the subsonic-flow range up to a mean inlet Mach number of about 0.8. When the diffuser is choked, shock losses cause a sharp increase in this value.

(2) For the thicker inlet boundary layer the total-pressure losses are about 5.5 porcent of inlet dynamic pressure at low-subsonic flow rates. Increasing flow rate causes an increase to about 9.5 percent before the configuration chokes. After choking, this value increases sharply.

(3) For the thinner inlet boundary layer, diffuser effectiveness, expressed as the ratio of actual-to-ideal static-pressure rise, is about 82.5 percent at low flow rates and decreases gradually with increasing flow rate to about 72.0 percent before choking. After choking, this value drops sharply.

(4) For the thicker inlet boundary layer, diffuser effectiveness is about 67.0 percent at low flow rates and decreases to about 55 percent beforo choking. After choking, this value drops sharply.

(5) Diffuser effectiveness, for both inlet boundary layers, is reduced more by failure to realize the theoretically possible drop in dynamic pressure than by losses incurred in converting the available change in dynamic pressure to change in static pressure. This is caused by the action of the boundary layer in reducing the effective expansion of the diffuser geometry.

(6) The boundary layer separates near the diffuser exit at very low flow rates for both inlet-boundary-layer configurations. The thicker-inlet-boundary-layer flow pattern is completely attachod at mean inlet Mach number of about 0.25 and remains attached until local separation in the high velocity flow around the transition curvature

disturbs the flow pattern at a mean inlet Mach number of about 0.80. The thinner-inlet-boundary-layer flow near the diffuser exit appears very unstable throughout the entire flow range, and some separation is present at all inlet Mach numbers.

Langley Aeronautical Laboratory
National Advisory Committee for Aeronautics
Langley Air Force Base, Va.

REFERENCES

1. Gibson, A. H.: On the Flow of Water through Pipes and Passages Having Converging or Diverging Boundaries. Proc. Roy. Soc. (London), ser. A, vol. 83, no. 563, March 2, 1910, pp. 366–378.

2. Squire, H. B.: Experiments on Conical Diffusers. Rep. No. Aero. 2216, British R.A.E., Aug. 1947.

3. Bohm, H., and Koppe, M.: The Influence of Friction on Steady Diffuser Flows at High Speed. Joint Intelligence Objectives Agency (Washington), July 23, 1946. (Also available from CADO, Wright-Patterson Air Force Base, as ATI No. 36689.)

4. Naumann: Wirkungsgrad von Diffusoren bei hohen Unterschallgeschwindigkeiten. FB Nr. 1705, Deutsche Luftfahrtforschung (Berlin – Adlershof), 1942.

5. Peters, H.: Conversion of Energy in Cross-Sectional Divergences under Different Conditions of Inflow. NACA TM 737, 1934.

6. Henry, John R.: Design of Power-Plant Installations. Pressure-Loss Characteristics of Duct Components. NACA ARR L4F26, 1944.

7. Patterson, G. N.: Modern Diffuser Design. Aircraft Engineering, vol. X, no. 115, Sept. 1938, pp. 267–273.

8. Copp, Martin R., and Klevatt, Paul L.: Investigation of High-Subsonic Performance Characteristics of a 12° 21-Inch Conical Diffuser, Including the Effects of Change in Inlet-Boundary-Layer Thickness. NACA RM L9H10, 1950.

9. Persh, Jerome: The Effect of the Inlet Mach Number and Inlet-Boundary-Layer Thickness on the Performance of a 23° Conical-Diffuser – Tail-Pipe Combination. NACA RM L9K10, 1950.

10. Merriam, Kenneth G., and Spaulding, Ellis R.: Comparative Tests of Pitot-Static Tubes. NACA TN 546, 1935.

11. Von Doenhoff, Albert E., and Tetervin, Neal: Determination of General Relations for the Behavior of Turbulent Boundary Layers. NACA Rep. 772, 1943.

Station	Distance from inlet (in.)	Diameter (in.)
1	-1.34	10.00
2	.22	10.05
3	4.26	10.90
4	7.41	11.56
5	11.85	12.50
6	15.79	13.32
7	20.10	14.14

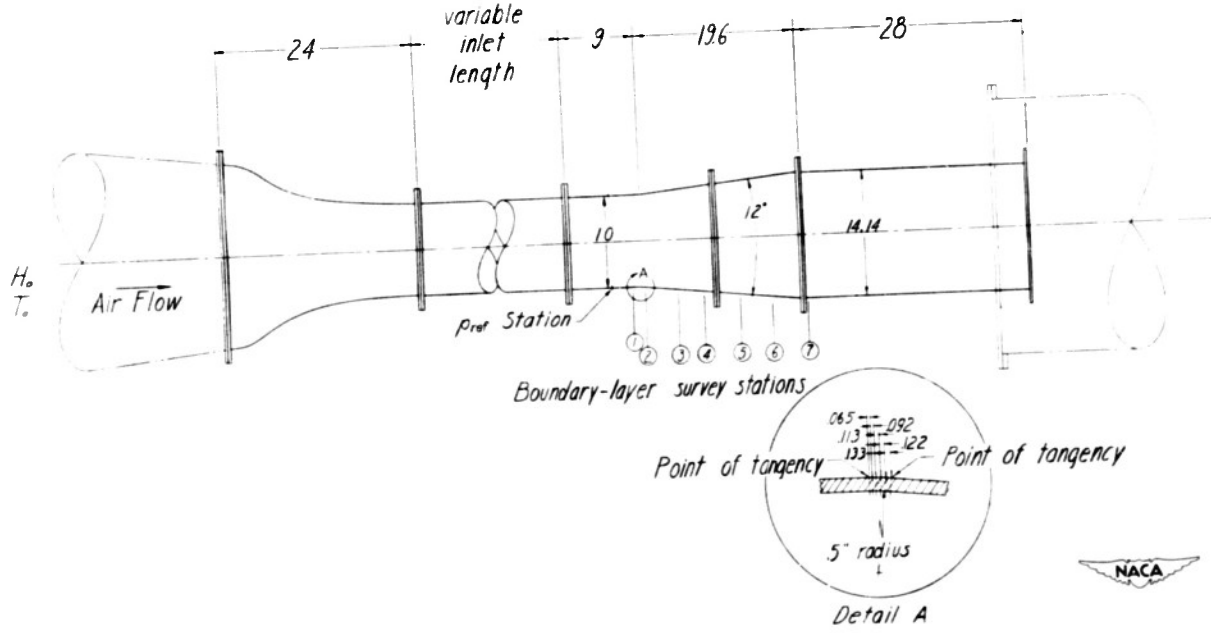

Figure 1.- Line drawing of apparatus. All dimensions are in inches.

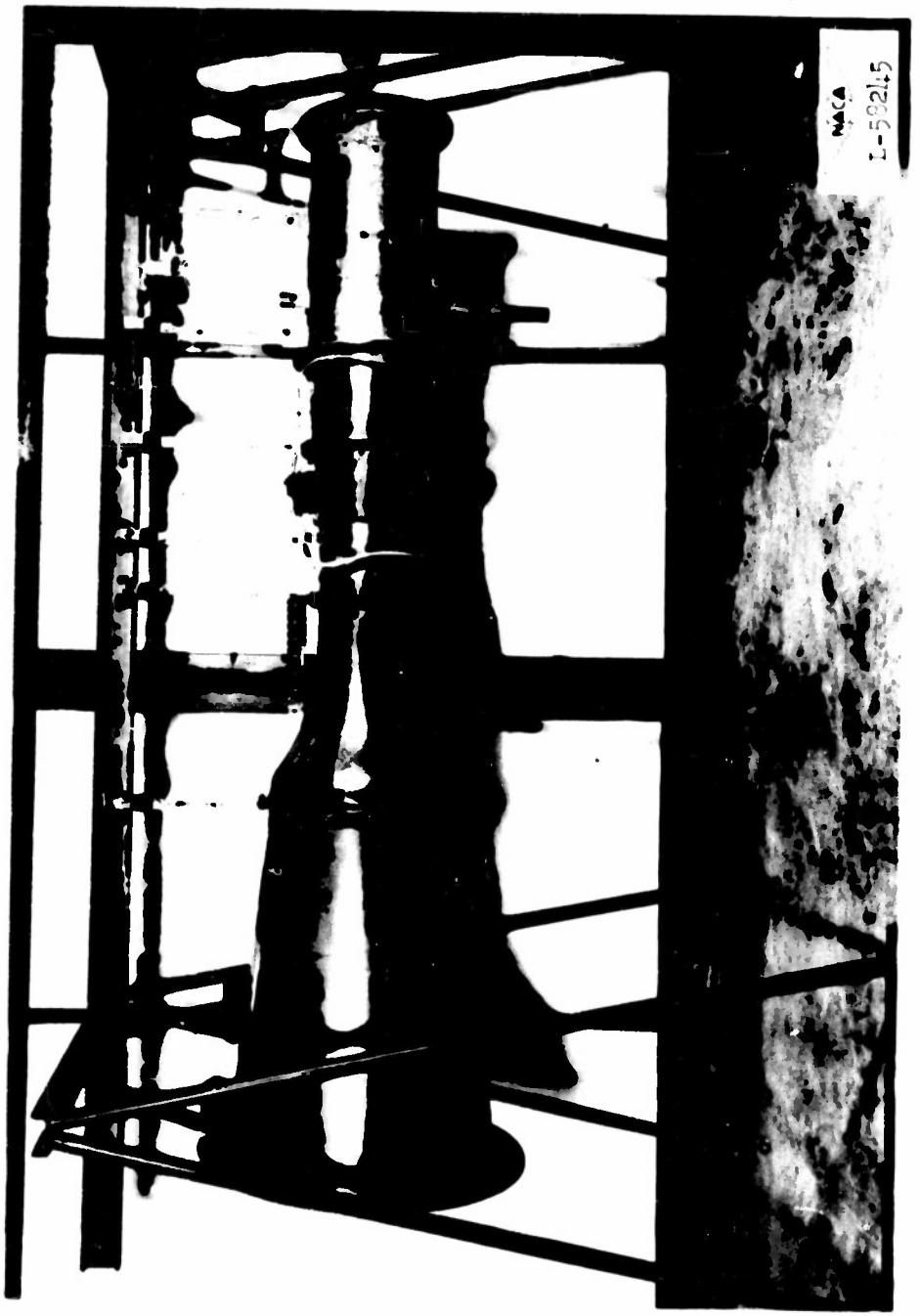

Figure 2.- Thinner-inlet-boundary-layer configuration.

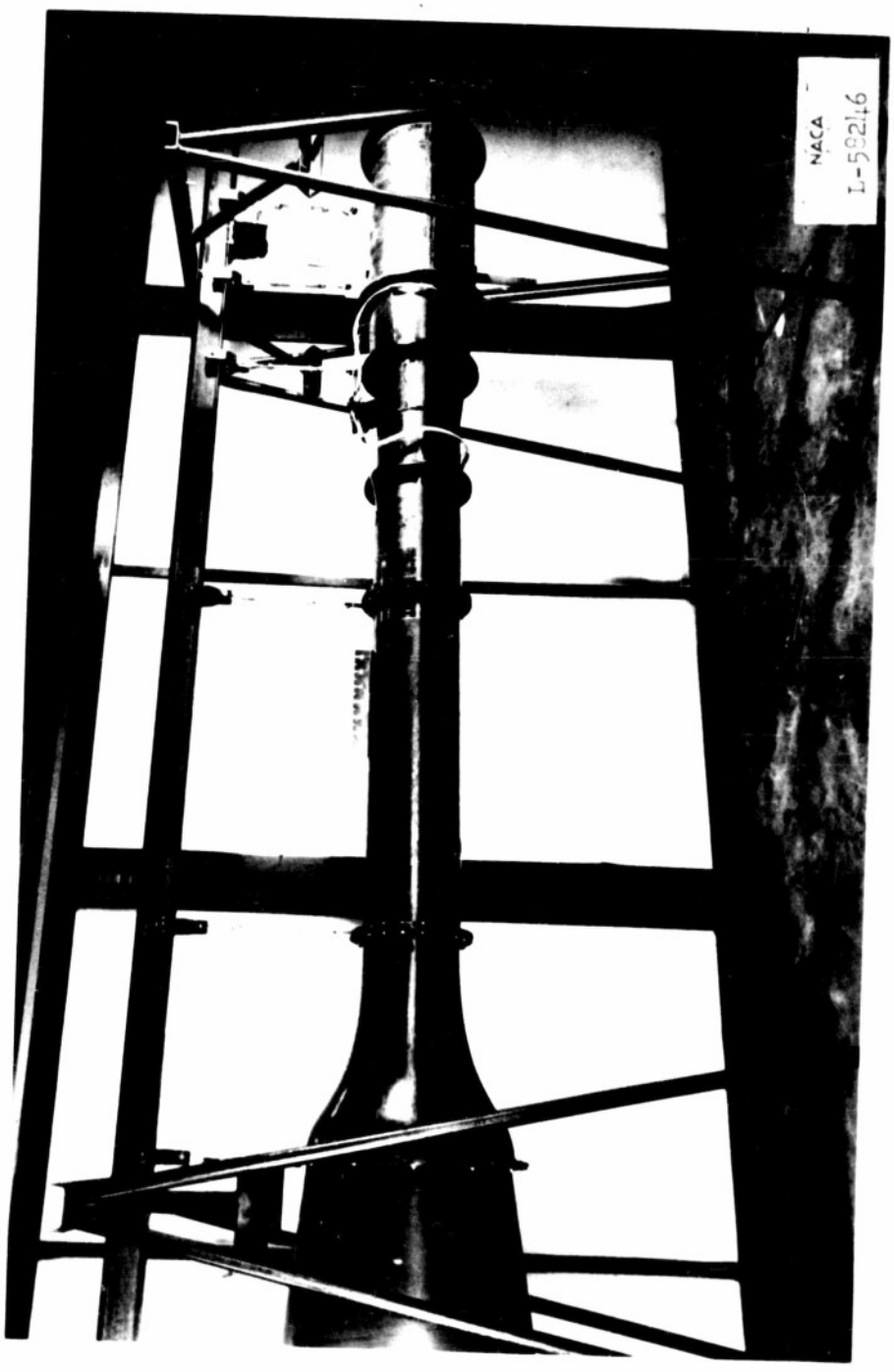

Figure 3.- Thicker-inlet-boundary-layer configuration.

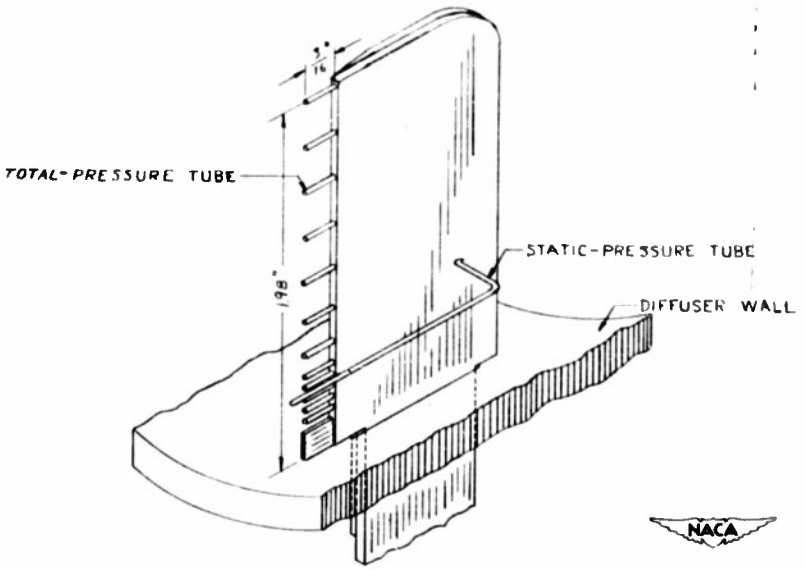

Figure 4.- Boundary-layer rake.

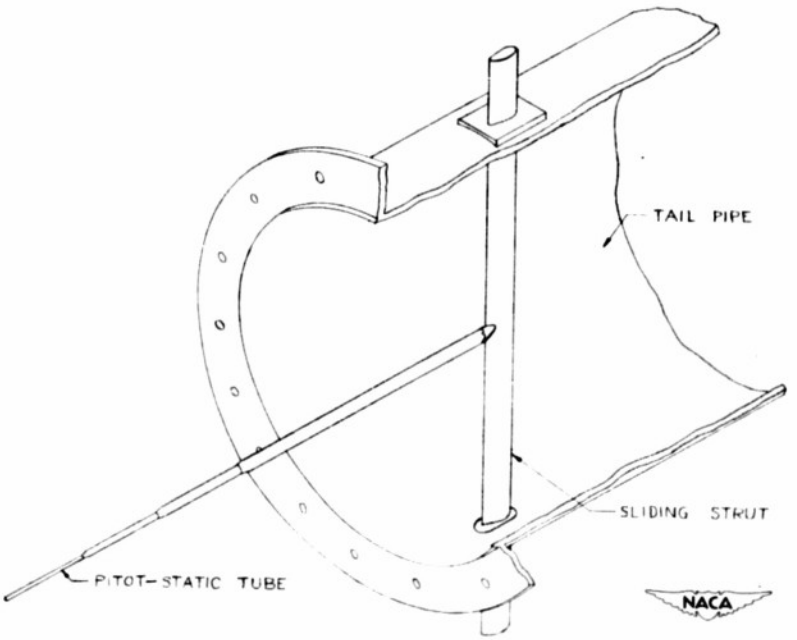

Figure 5.- Survey tube.

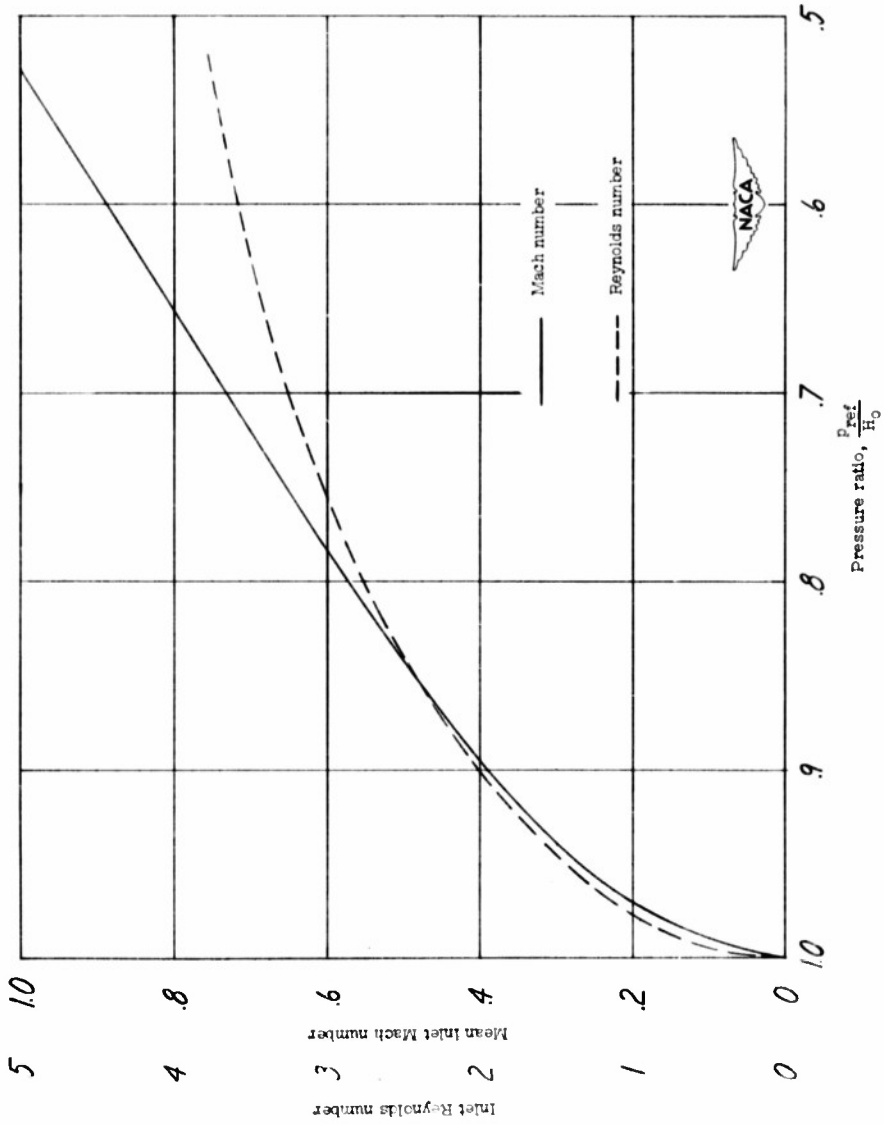

Figure 6.- Variation of mean inlet Mach number at the P_{ref} station with the correlating pressure ratio $\frac{P_{ref}}{H_o}$.

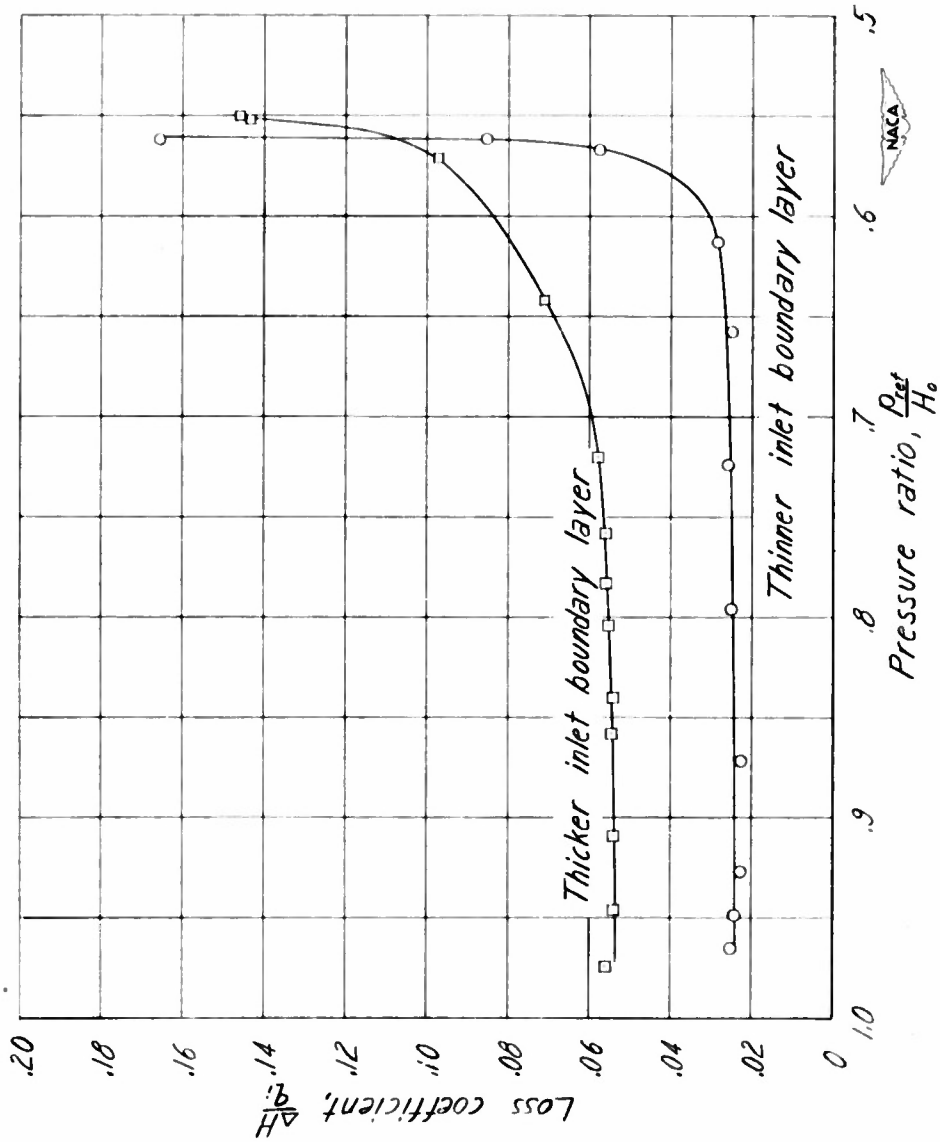

Figure 7.- Variation of loss coefficient with pressure ratio.

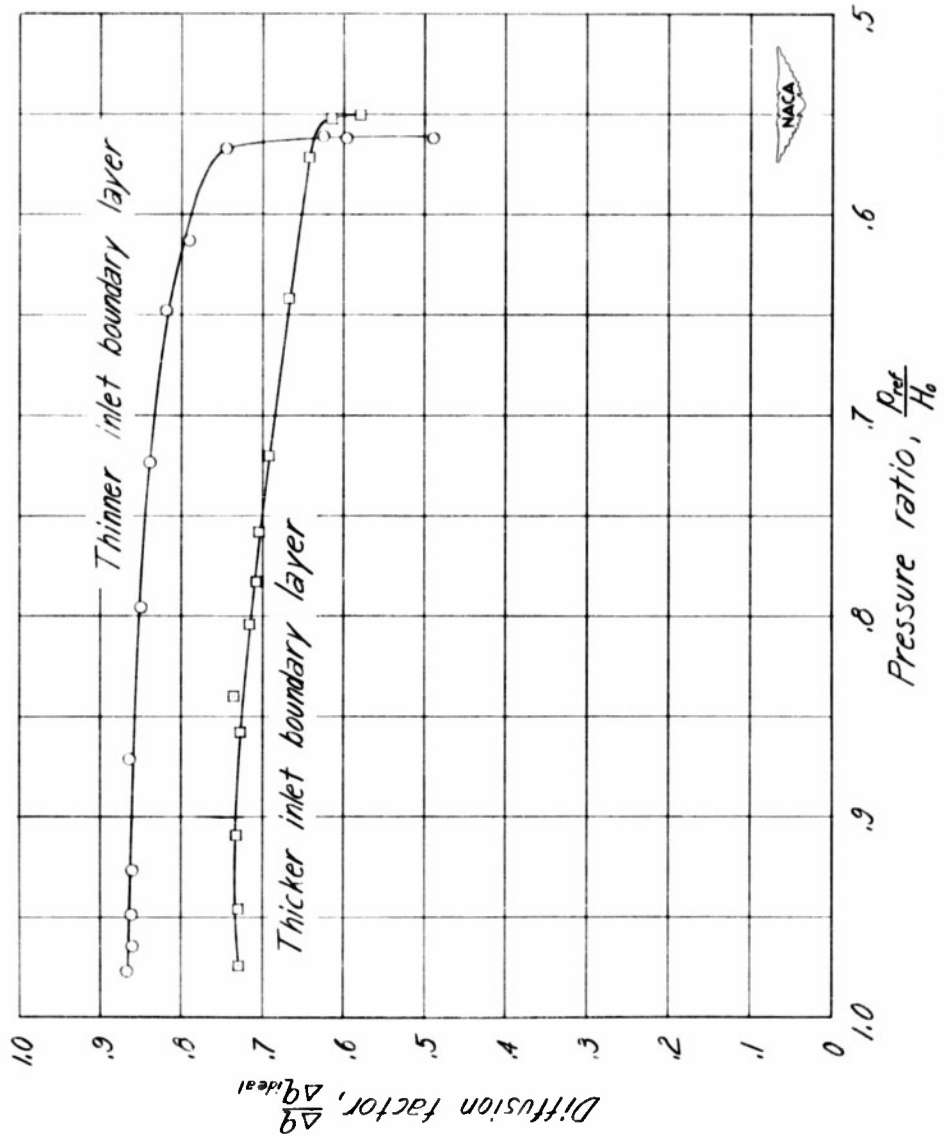

Figure 8.- Variation of diffusion factor with pressure ratio.

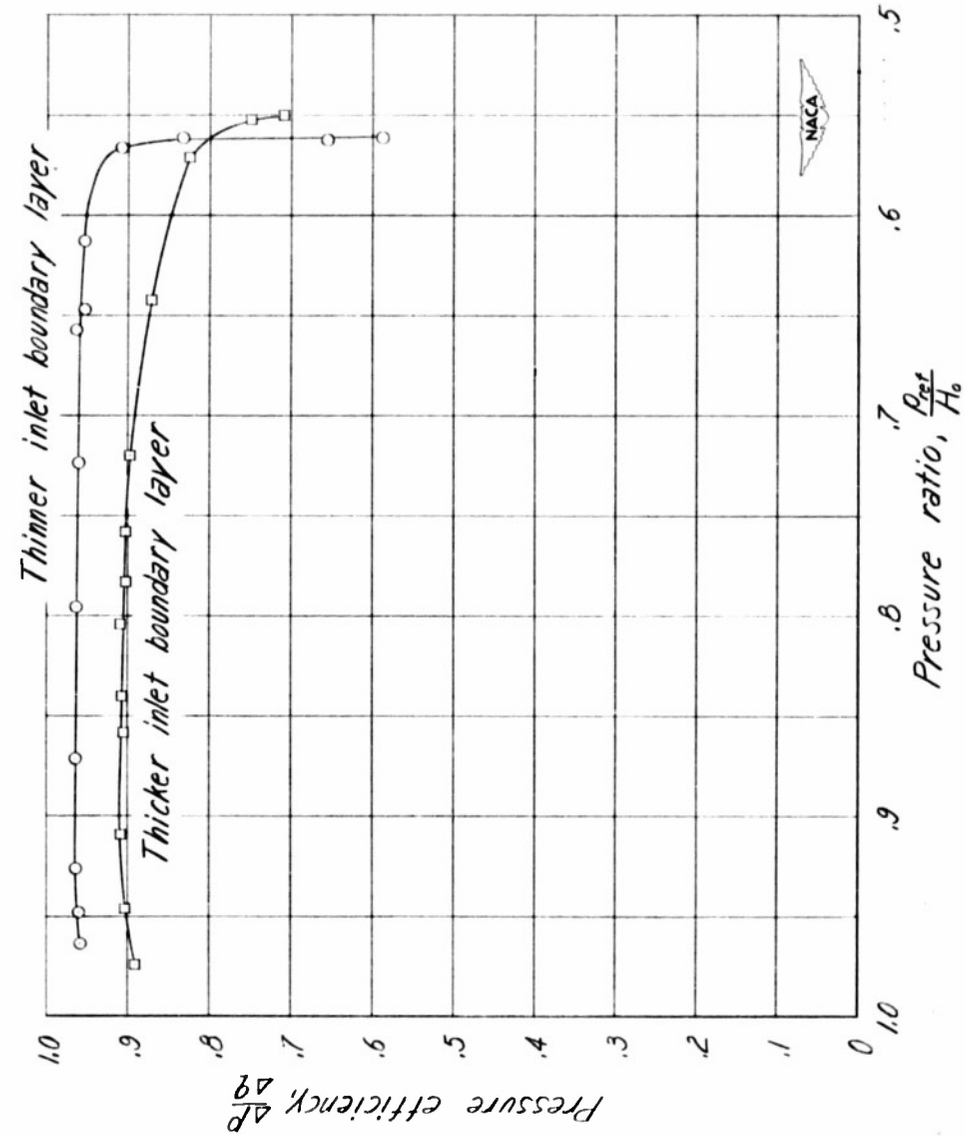

Figure 9.- Variation of pressure efficiency with pressure ratio.

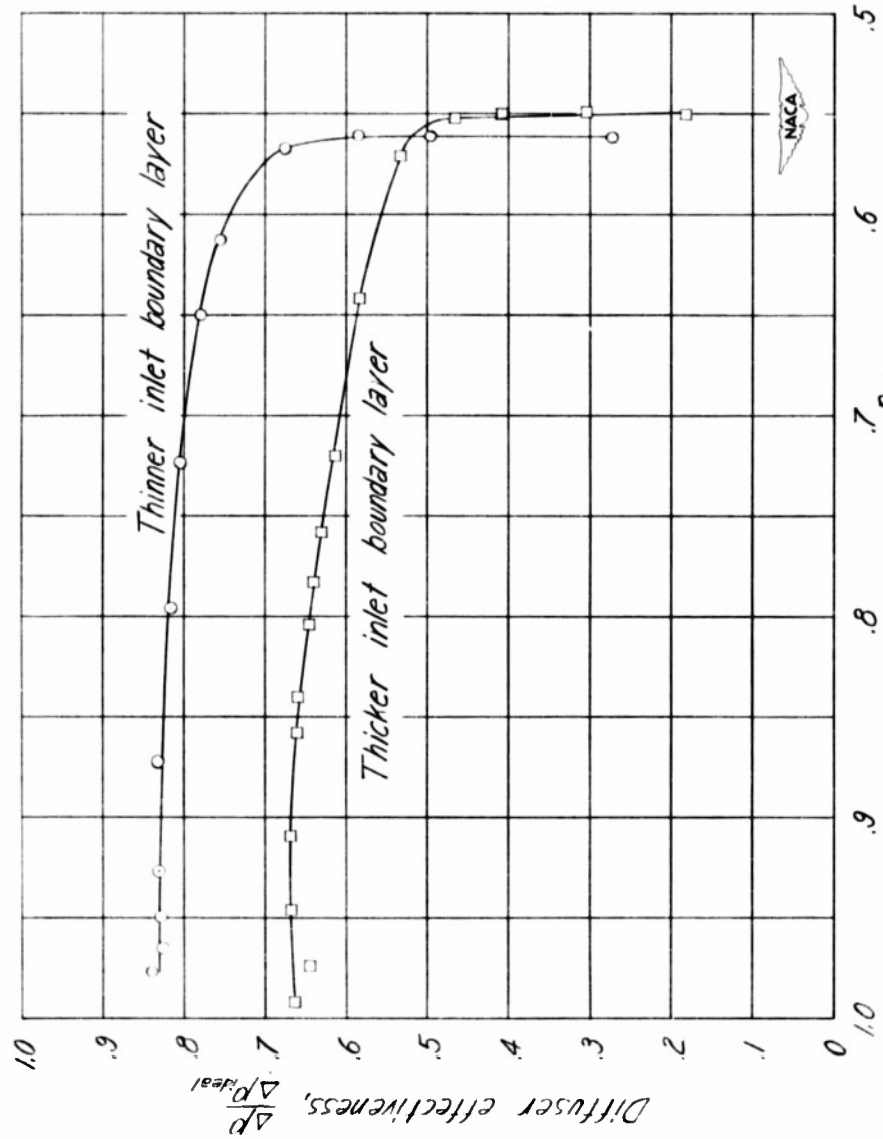

Figure 10.- Variation of diffuser effectiveness with pressure ratio.

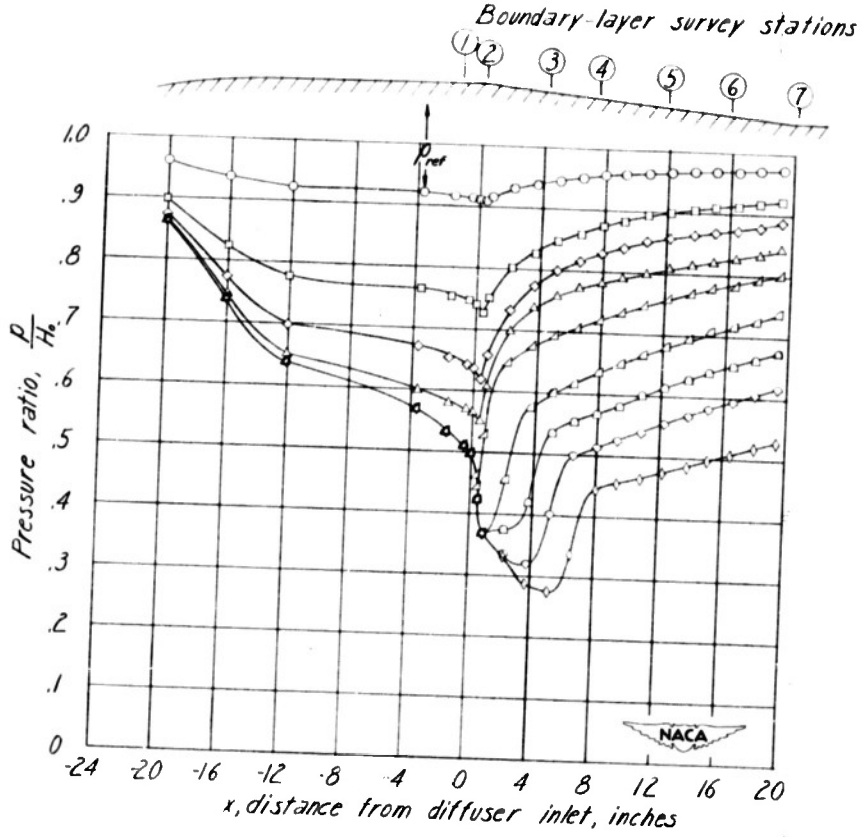

Figure 11.- Static-pressure distribution - thinner inlet boundary layer.

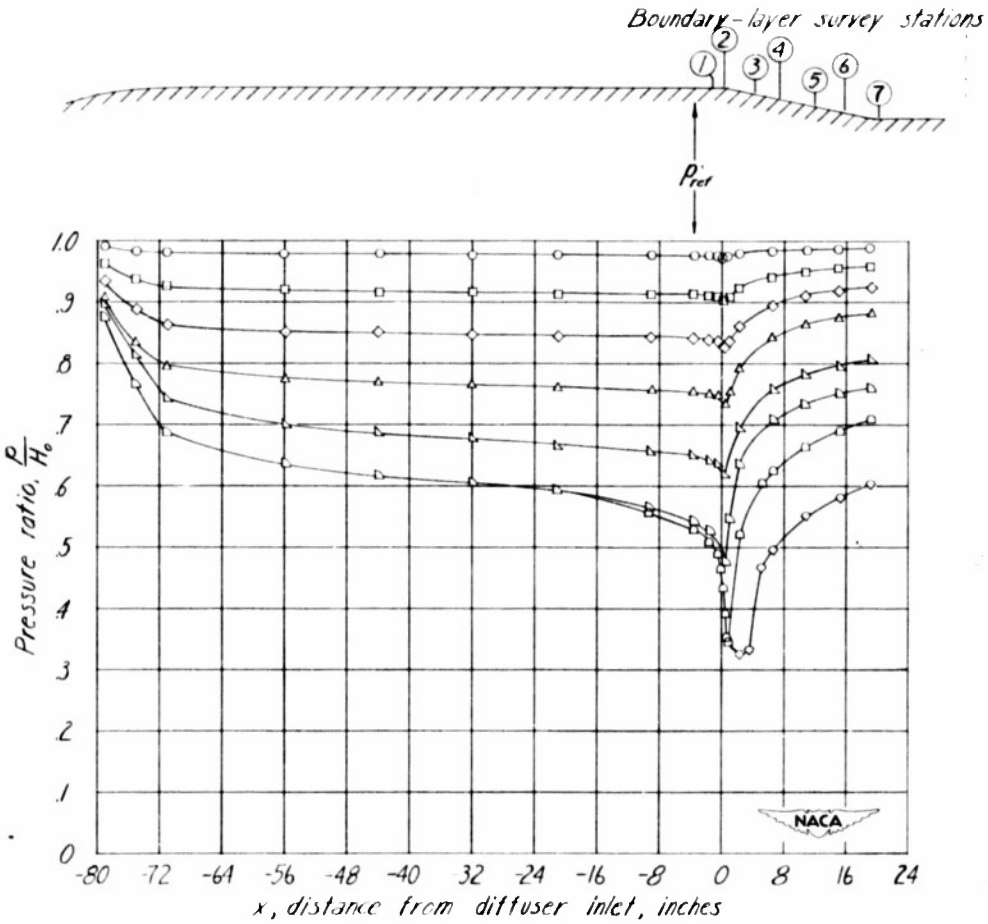

Figure 12.- Static-pressure distribution - thicker inlet boundary layer.

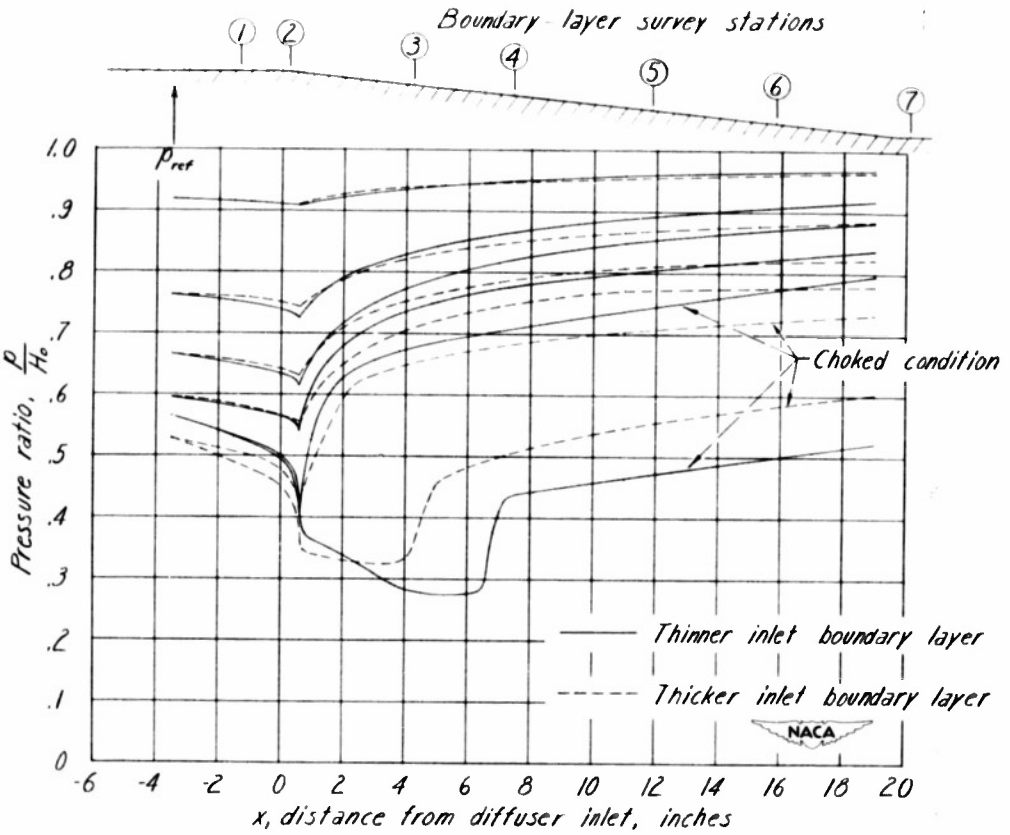

Figure 13.- Comparison of static-pressure distribution.

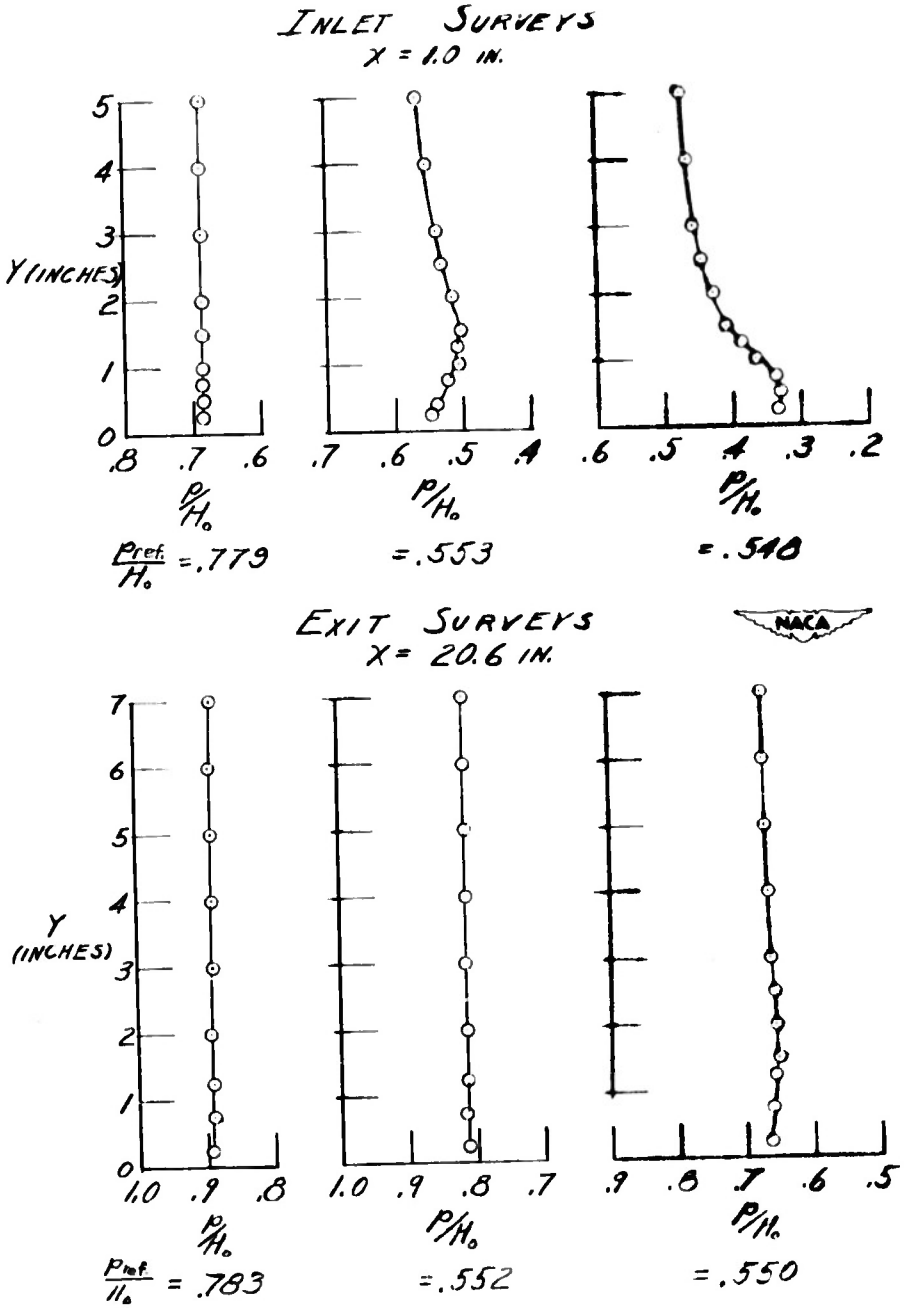

Figure 14.- Radial static-pressure distributions - thinner inlet boundary layer.

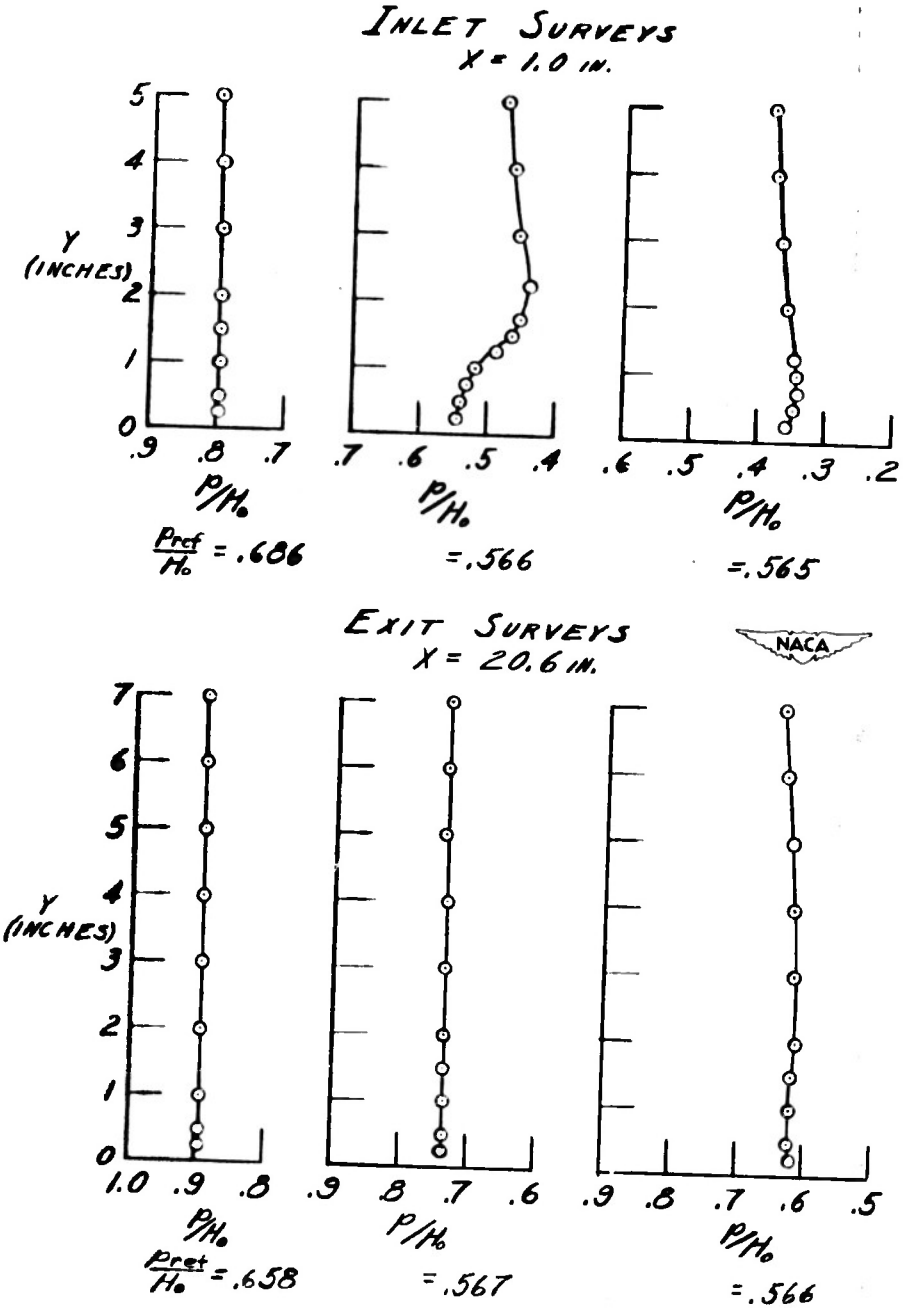

Figure 15.- Radial static-pressure distributions - thicker inlet boundary layer.

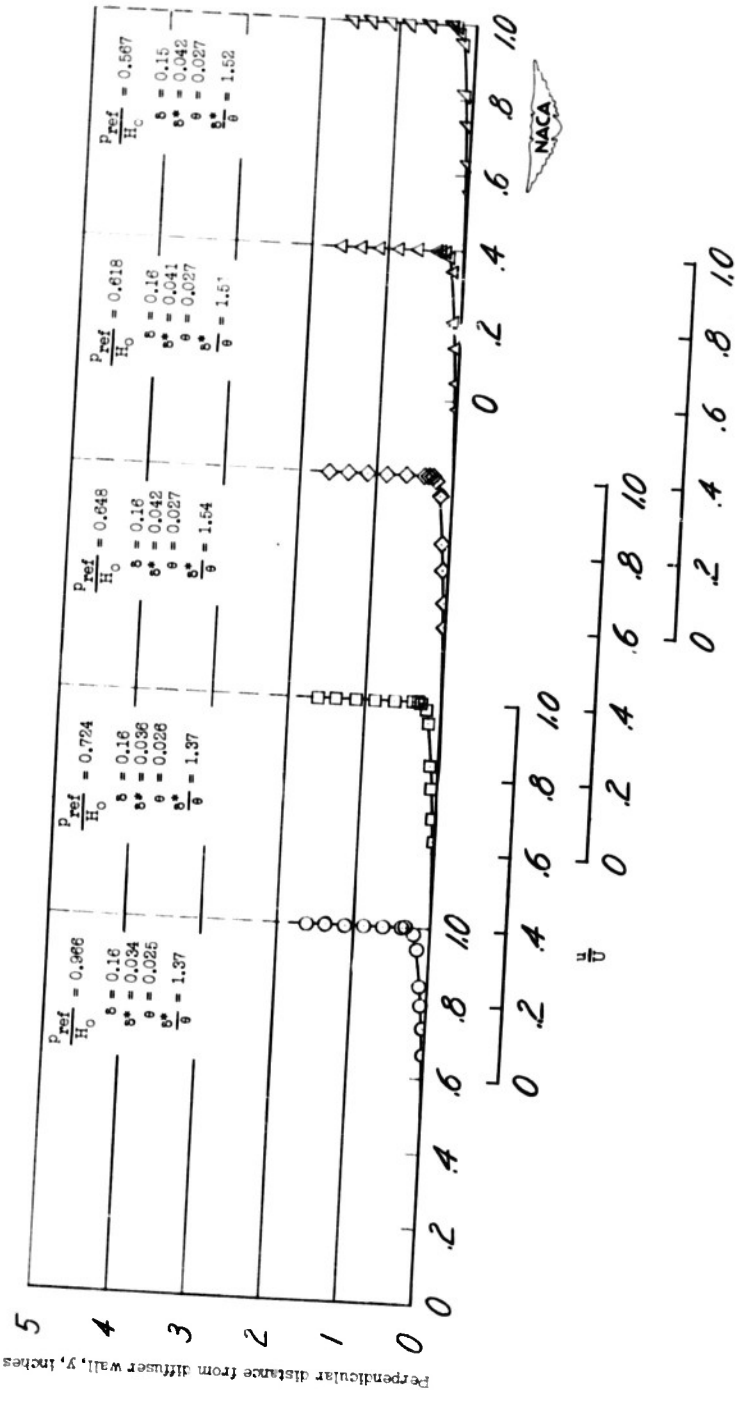

(a) Station 1.

Figure 16.- Boundary-layer profiles - thinner inlet boundary layer.

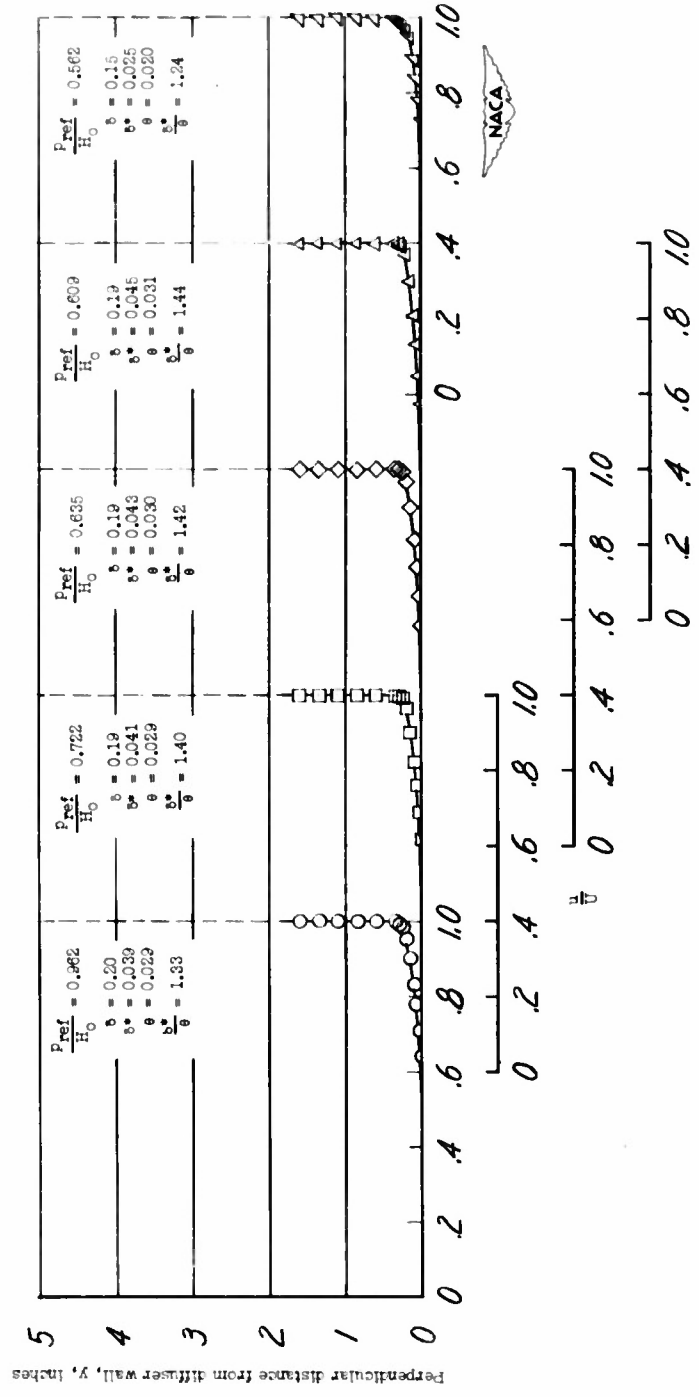

(b) Station 2.

Figure 16.- Continued.

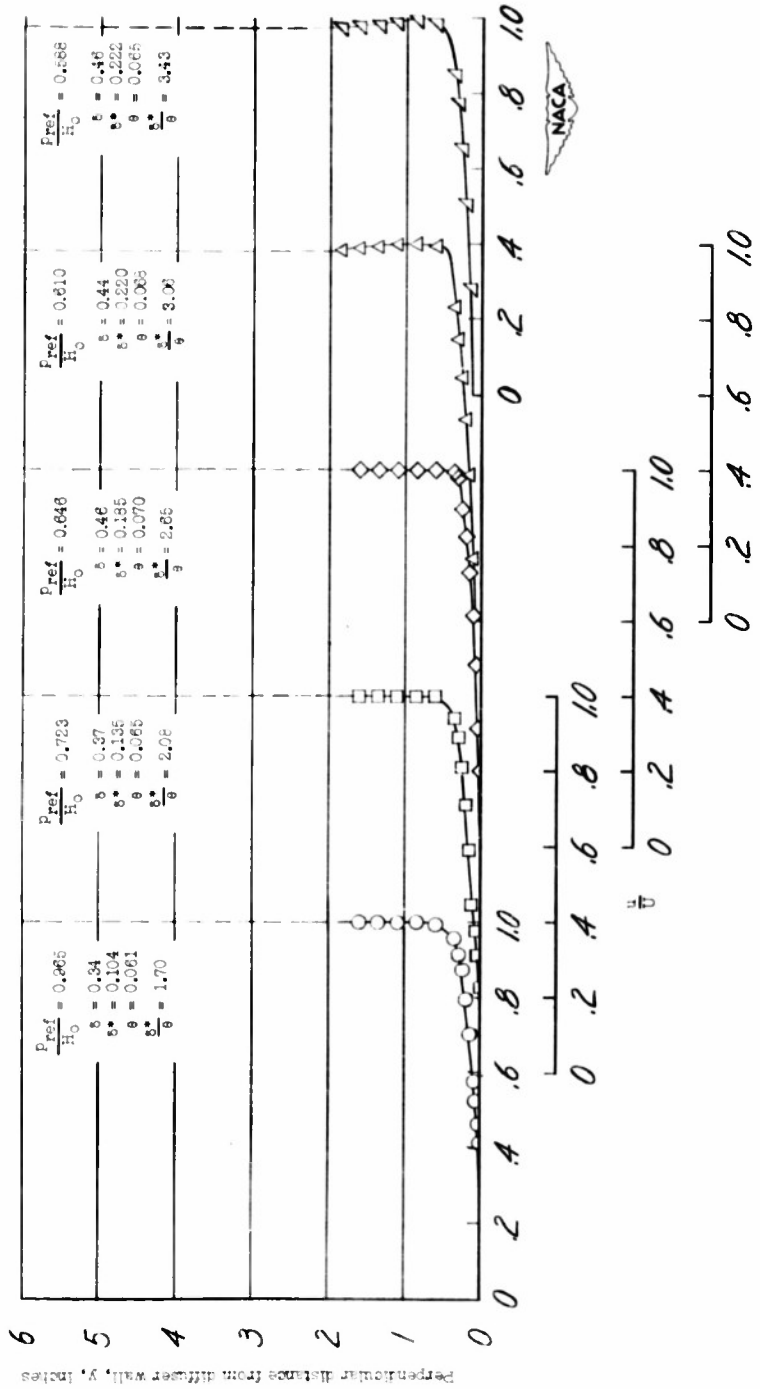

(c) Station 3.

Figure 16.- Continued.

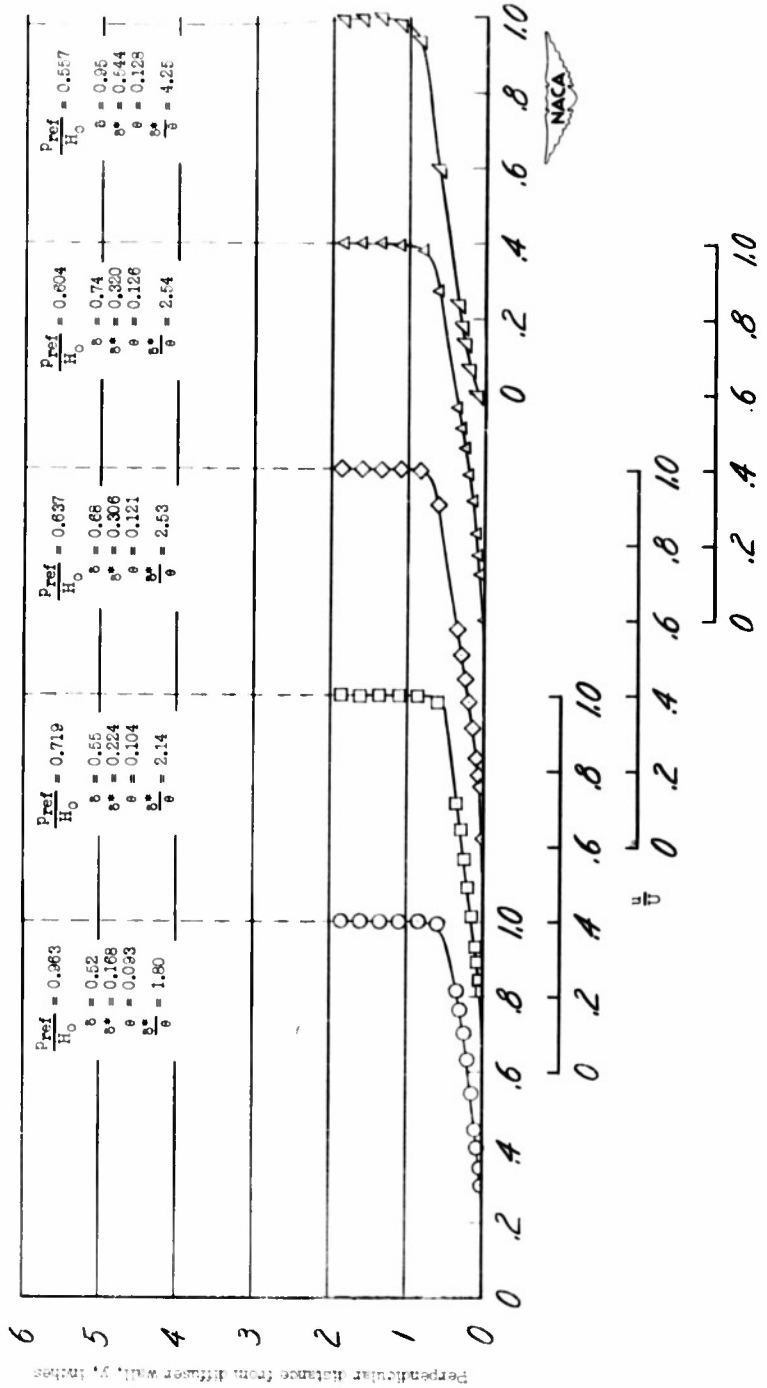

(d) Station 4.

Figure 16.- Continued.

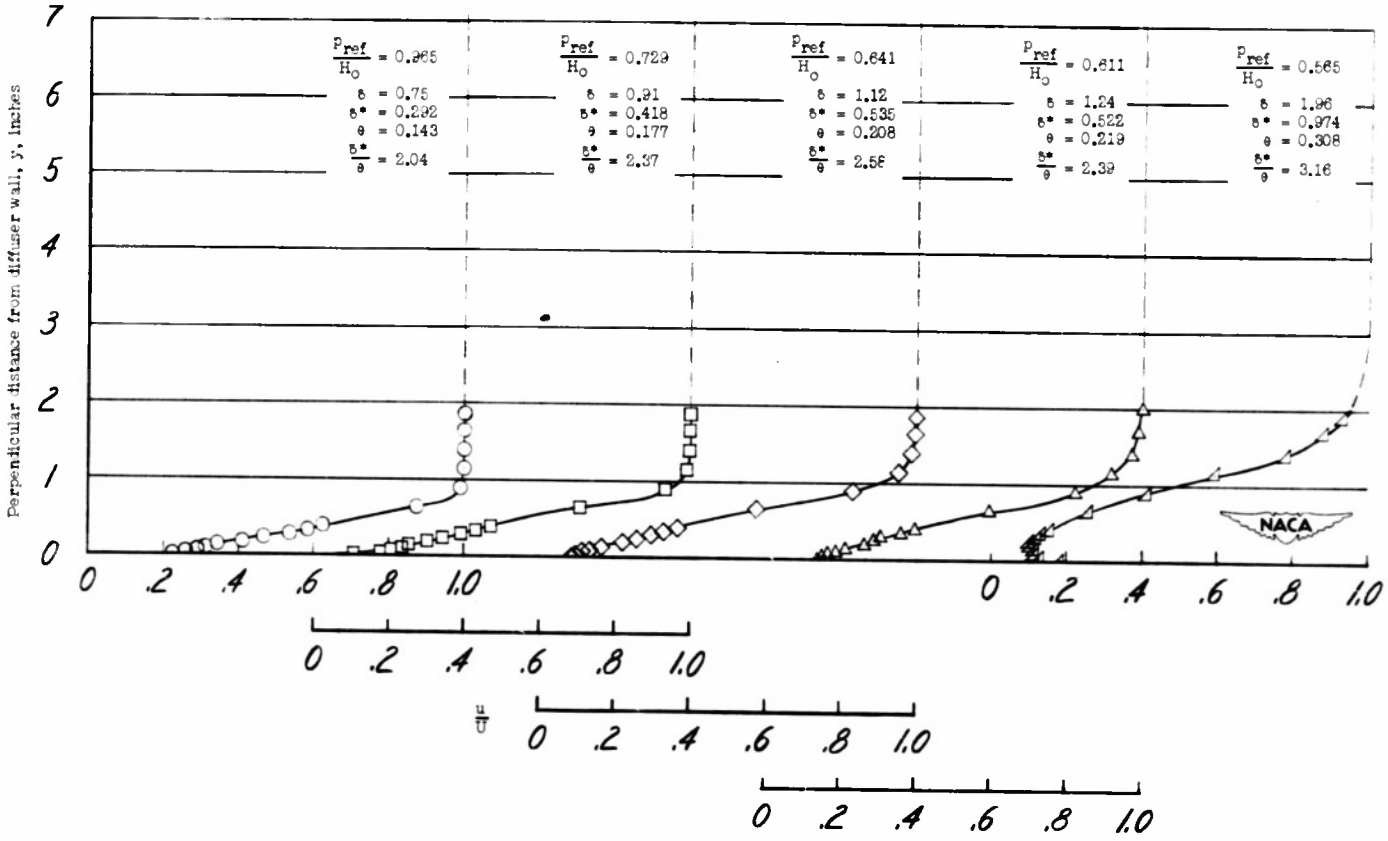

(e) Station 5.

Figure 16.- Continued.

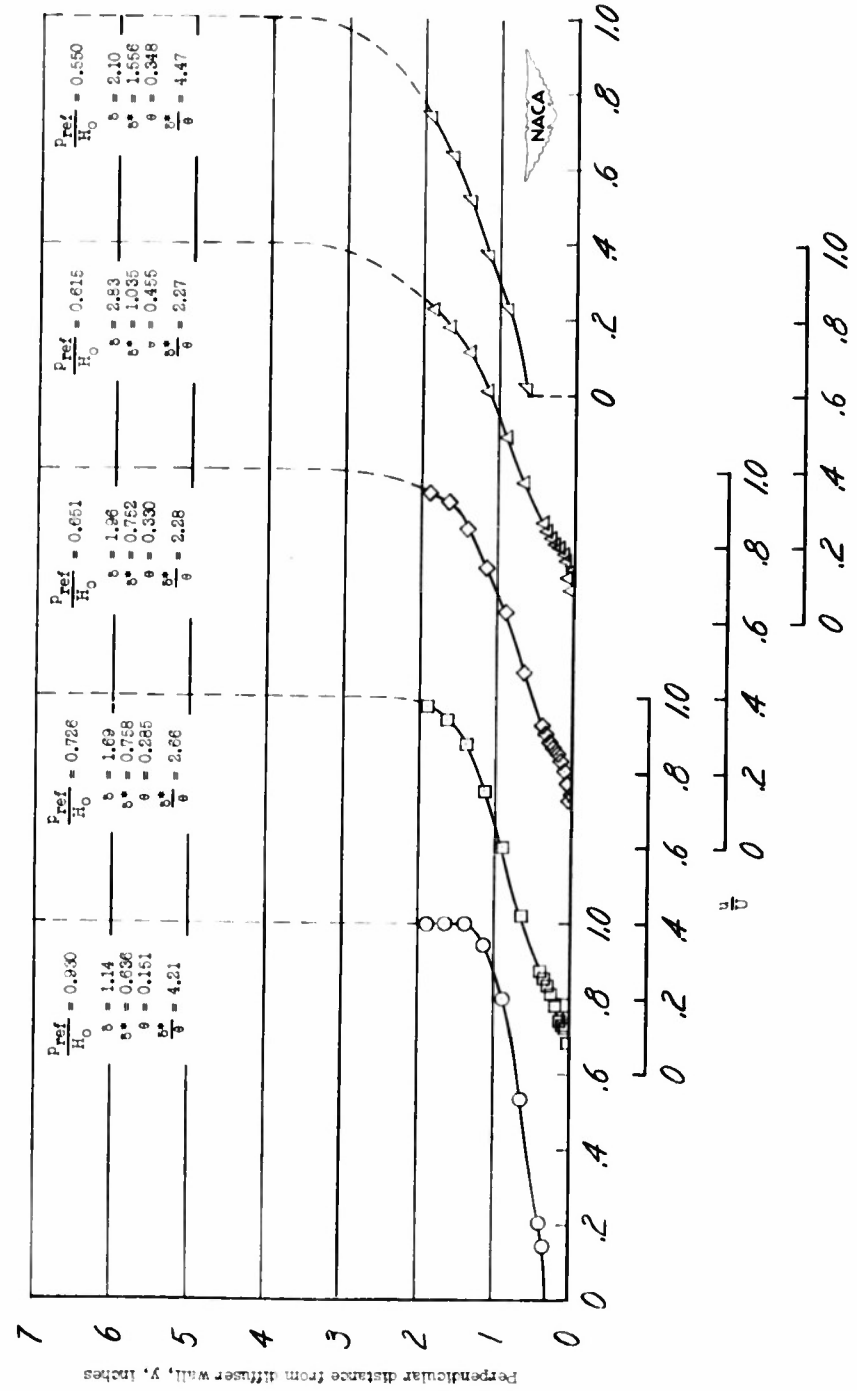

(f) Station 6.

Figure 16.- Continued.

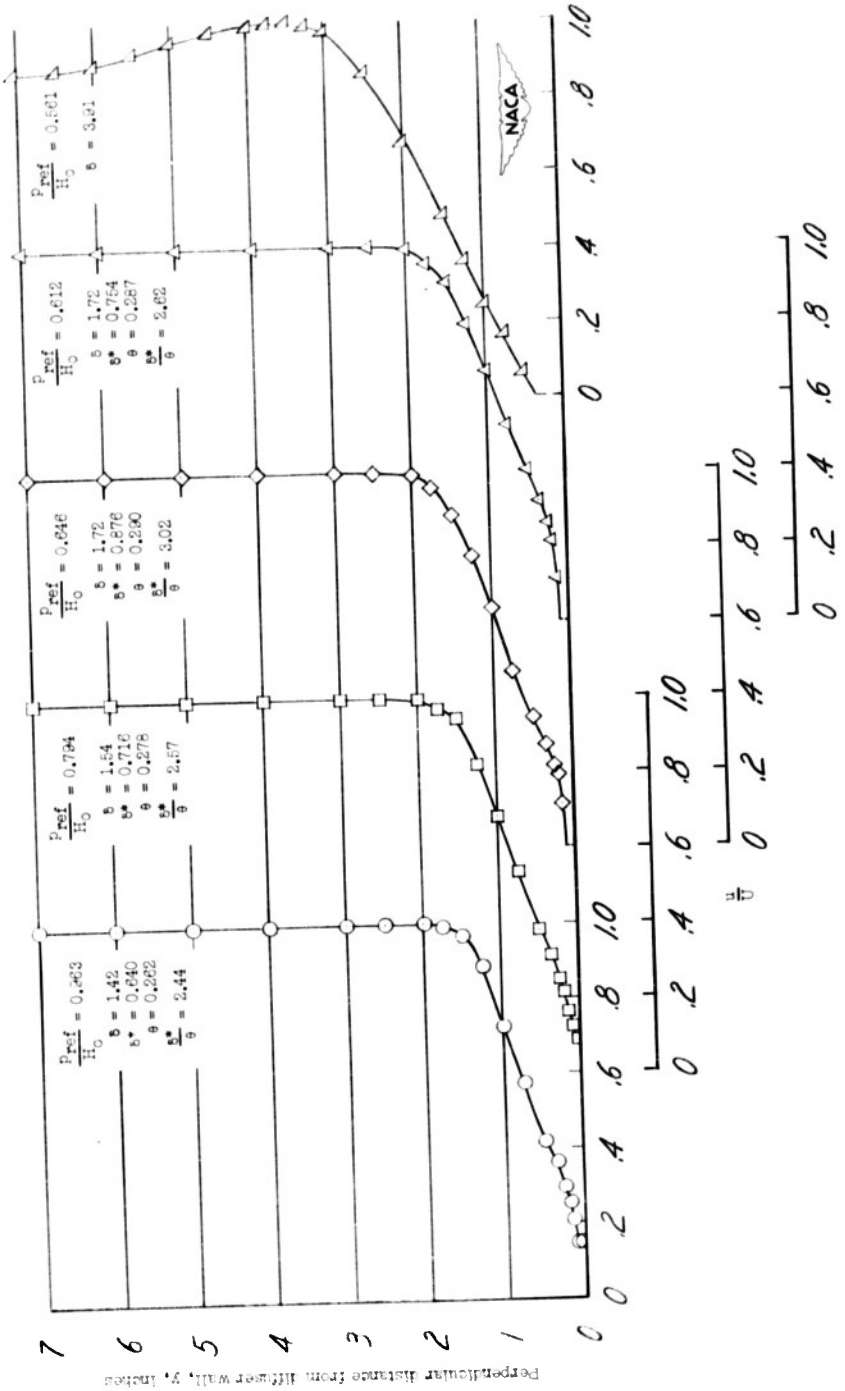

(g) Station 7.

Figure 16.- Concluded.

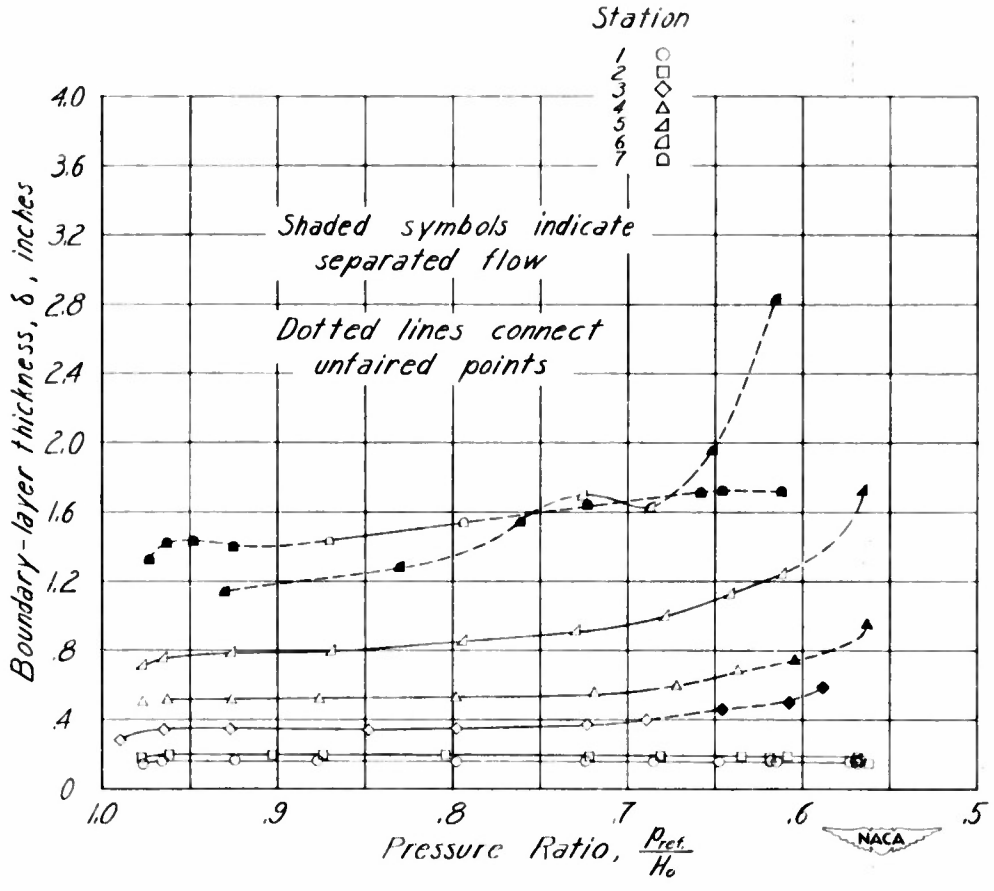

Figure 17.- Variation of boundary-layer thickness with pressure ratio - thinner inlet boundary layer.

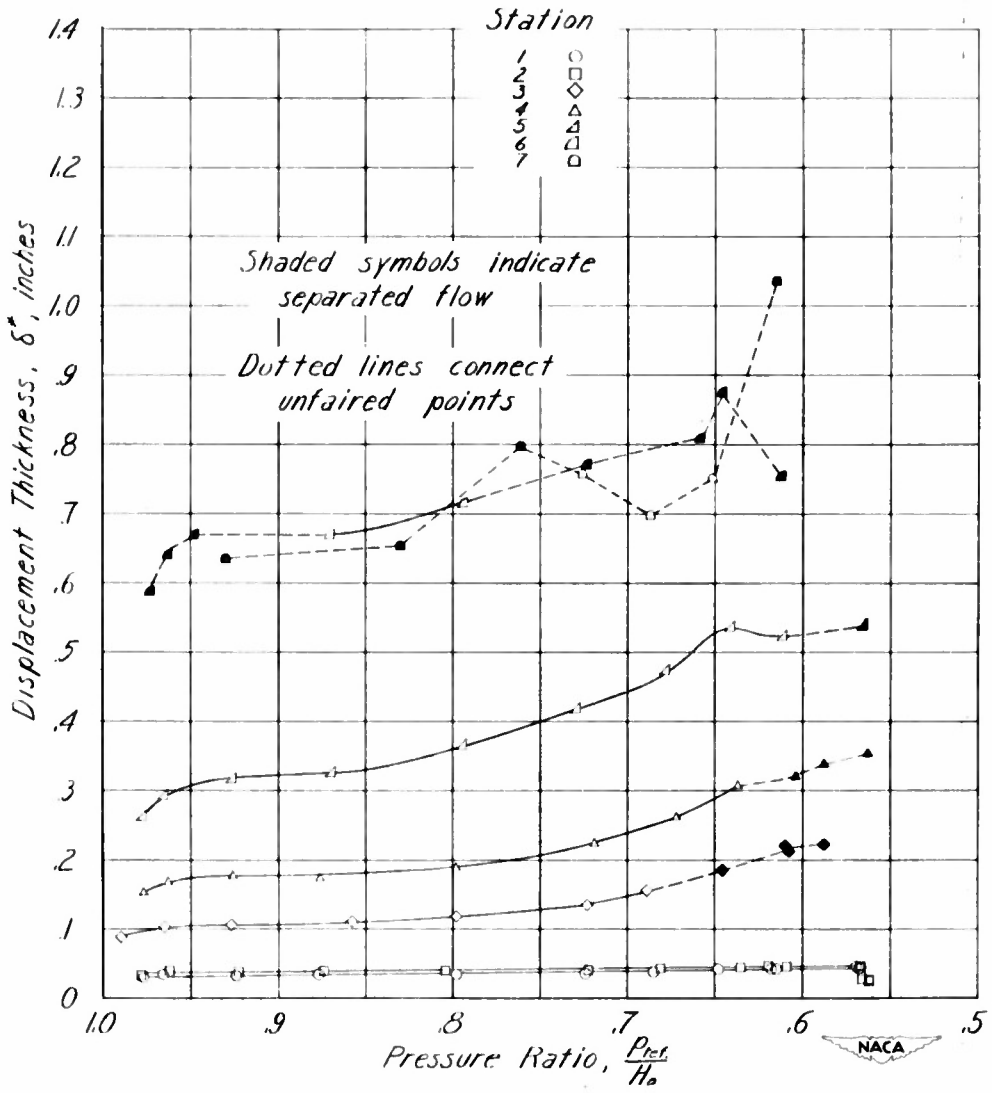

Figure 18.- Variation of displacement thickness with pressure ratio - thinner inlet boundary layer.

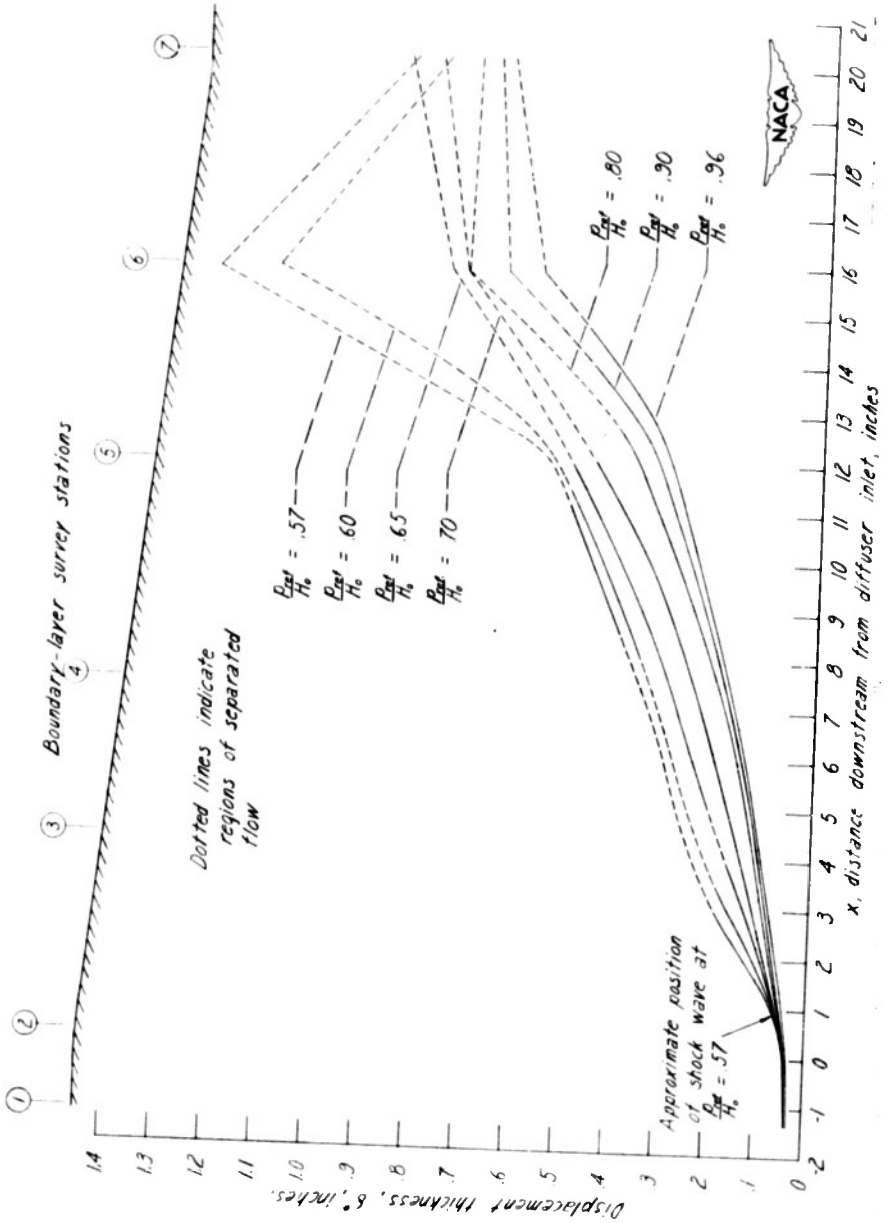

Figure 19.- Growth of displacement thickness in the thinner-inlet-boundary-layer diffuser.

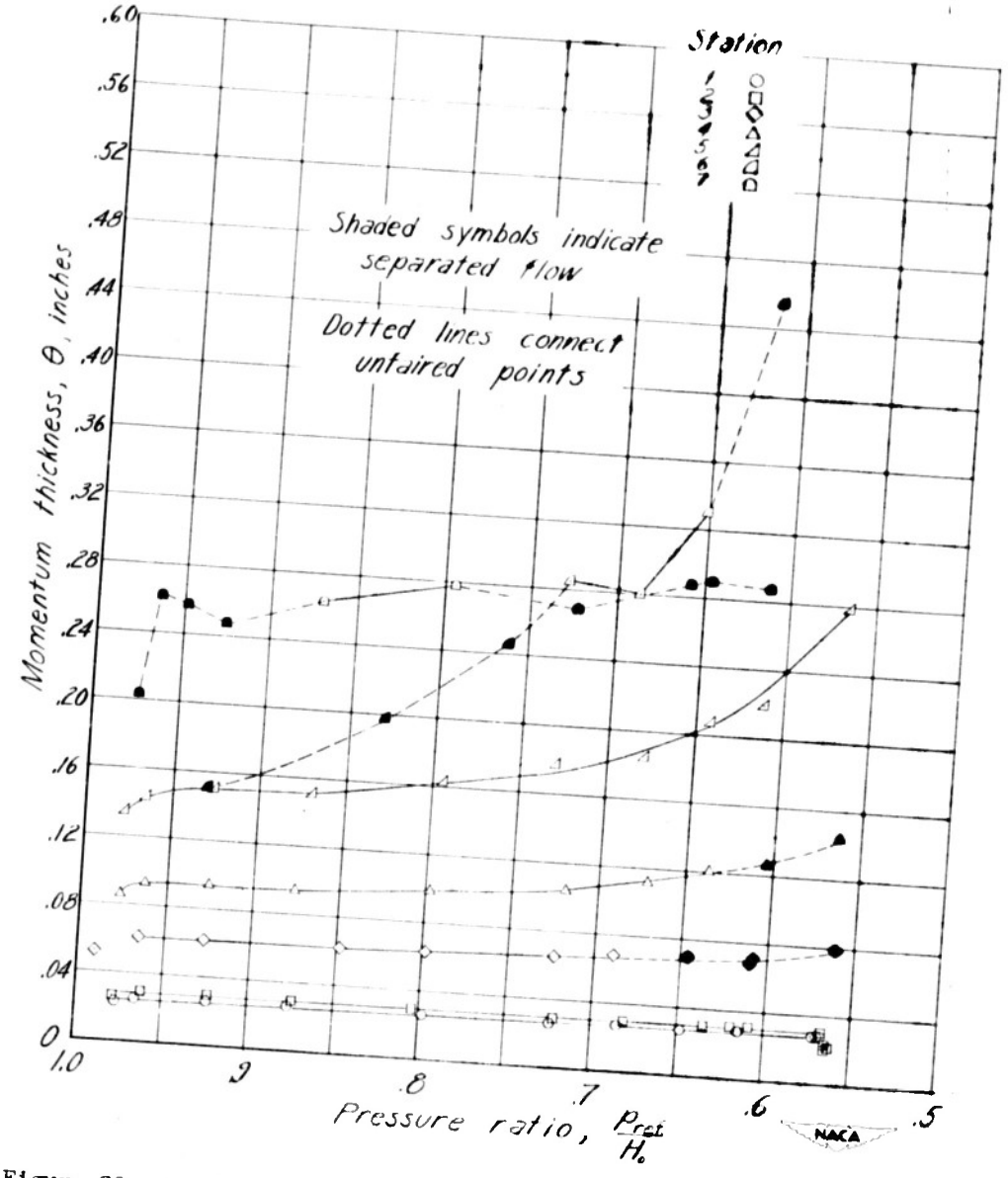

Figure 20.- Variation of momentum thickness with pressure ratio - thinner inlet boundary layer.

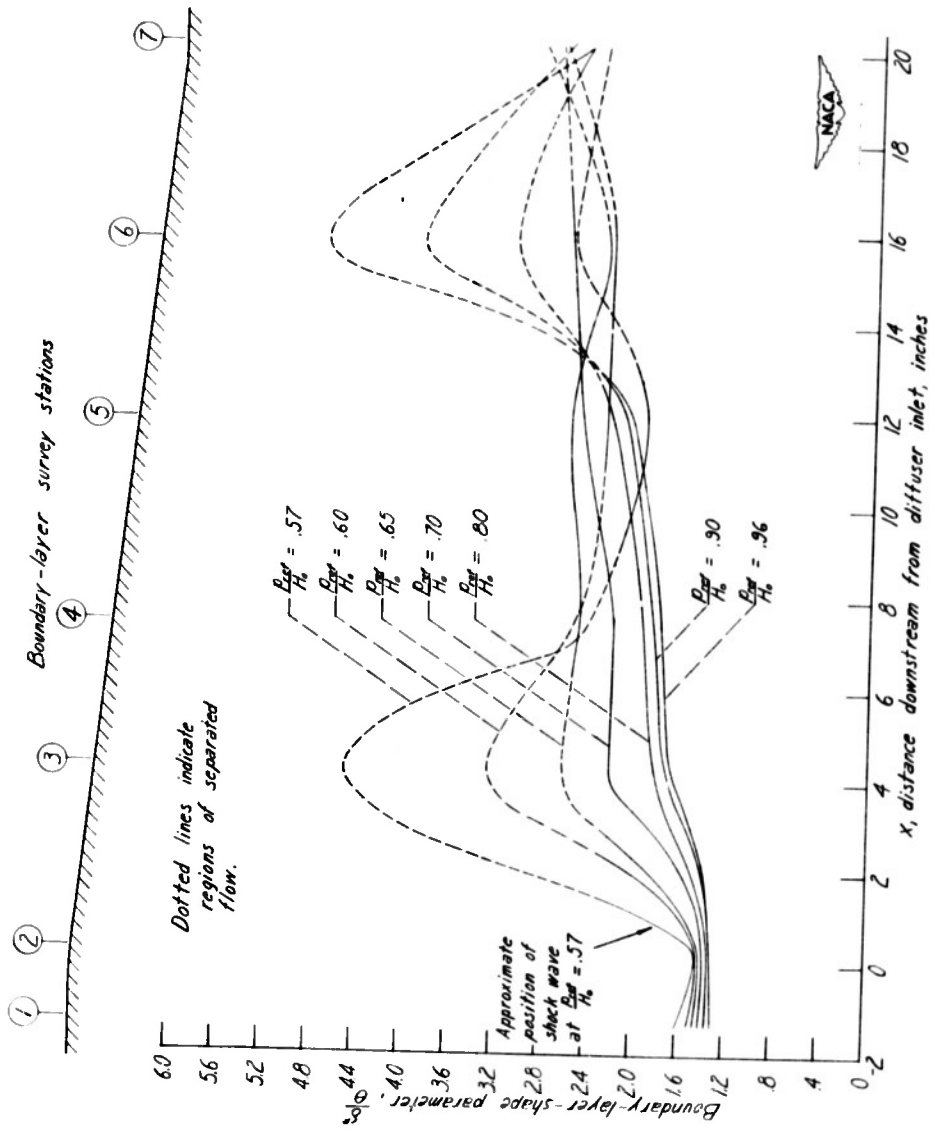

Figure 23.- Growth of boundary-layer-shape parameter in the thinner-inlet-boundary-layer diffuser.

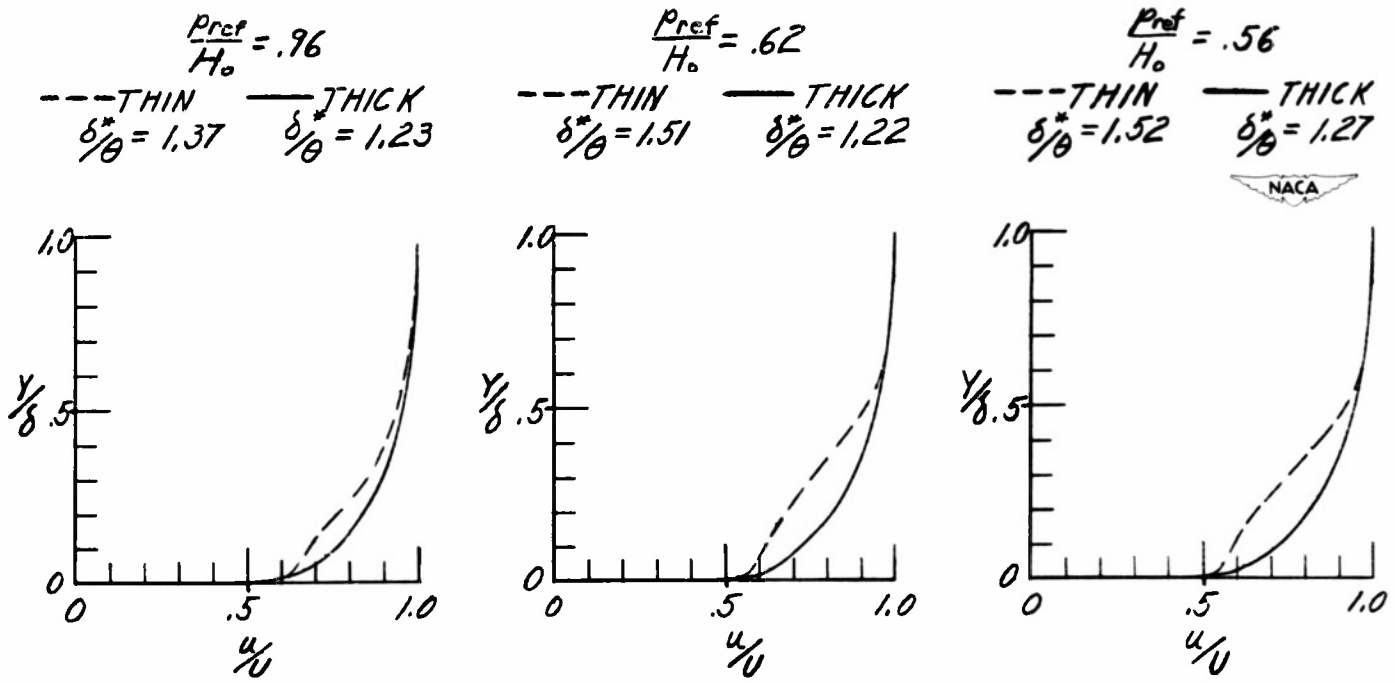

Figure 24.- Comparison of nondimensional velocity profiles at boundary-layer station 1.

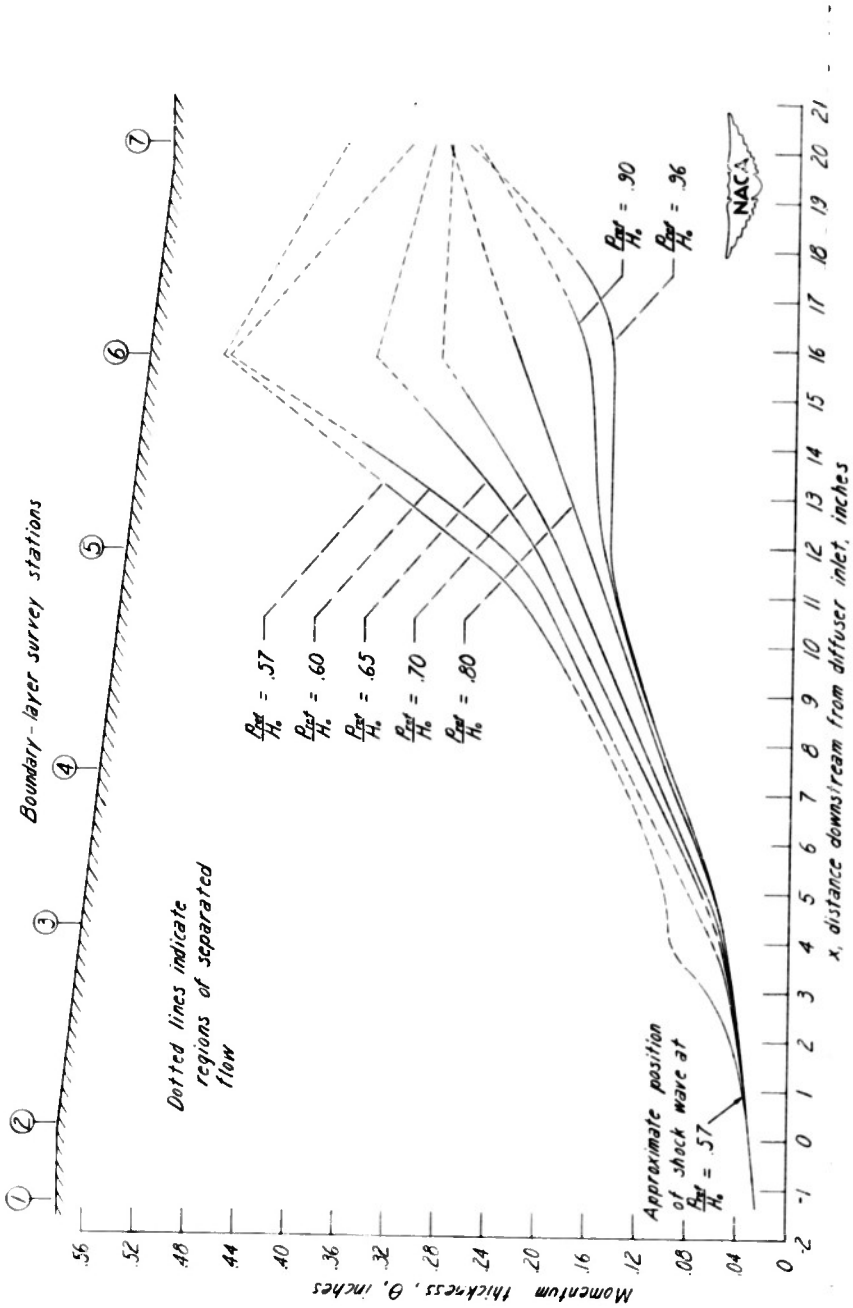

Figure 21.- Growth of momentum thickness in the thinner-inlet-boundary-layer diffuser.

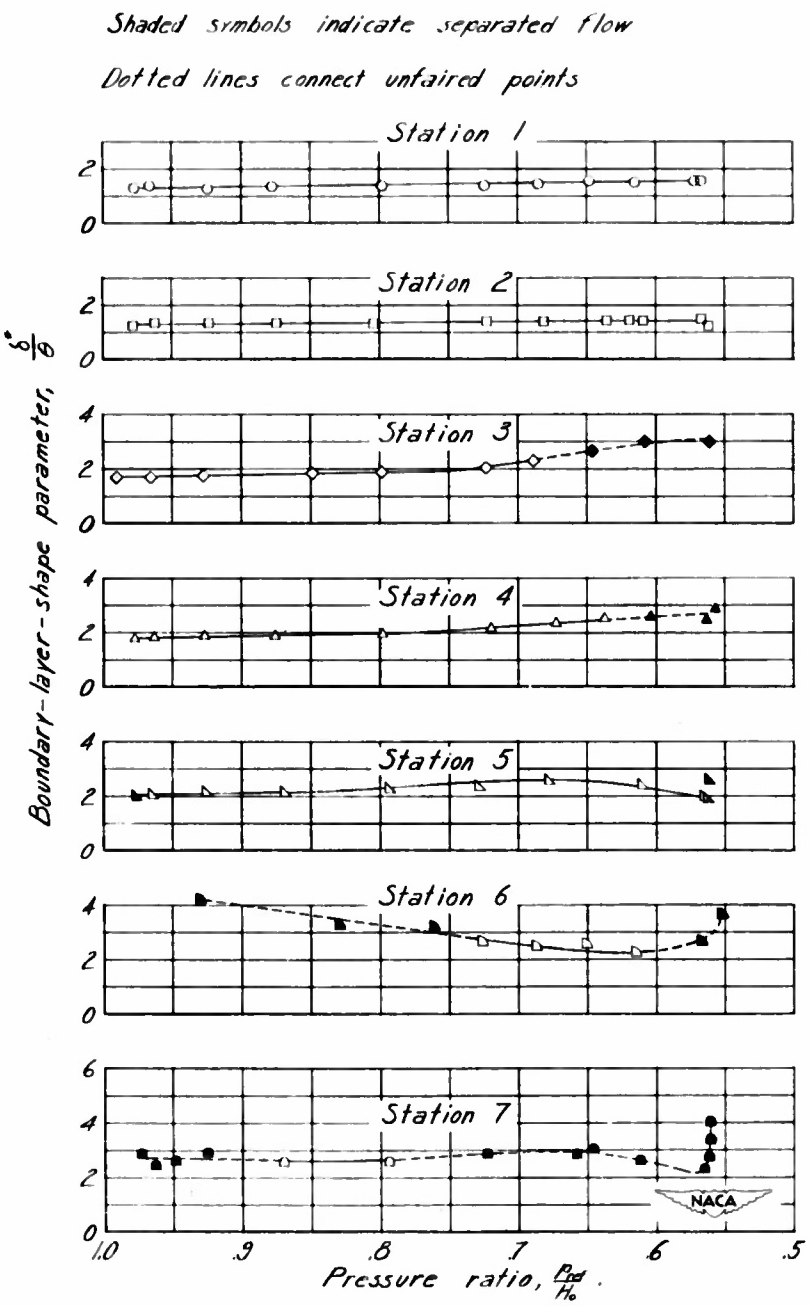

Figure 22.- Variation of boundary-layer-shape parameter with pressure ratio - thinner inlet boundary layer.

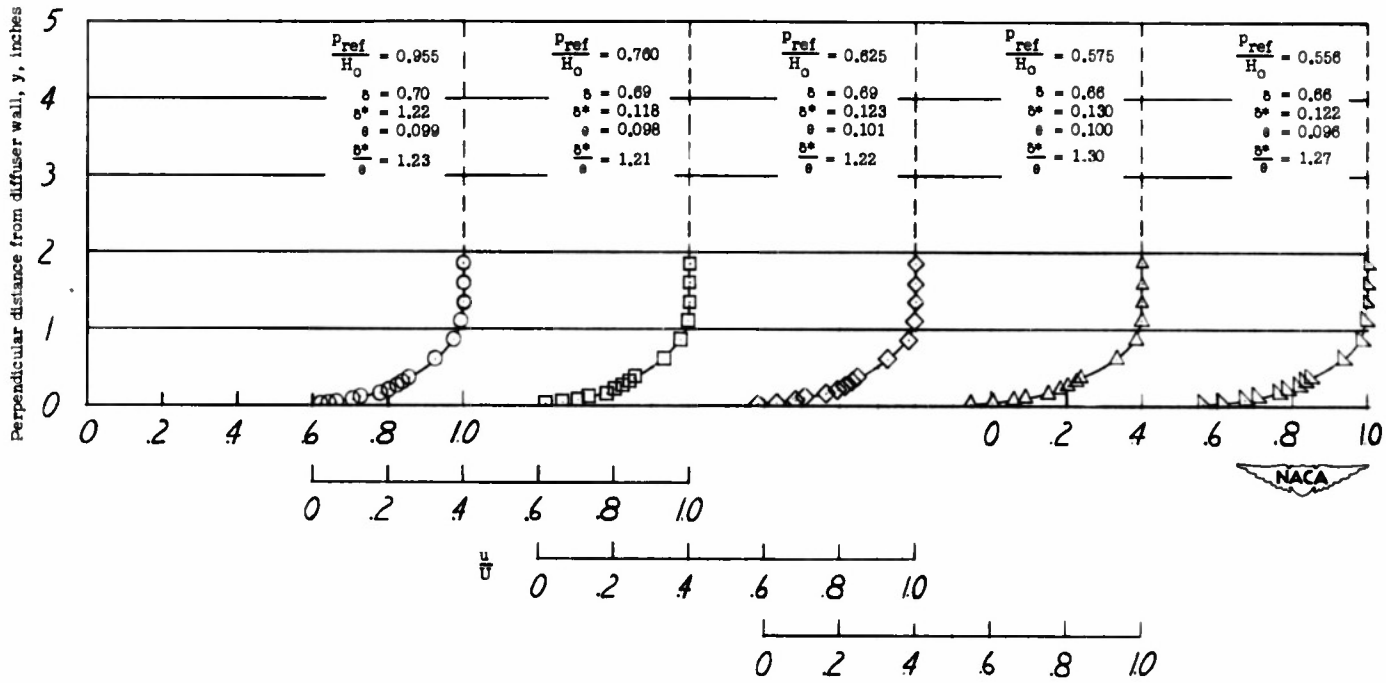

(a) Station 1.

Figure 25.- Boundary-layer profiles - thicker inlet boundary layer.

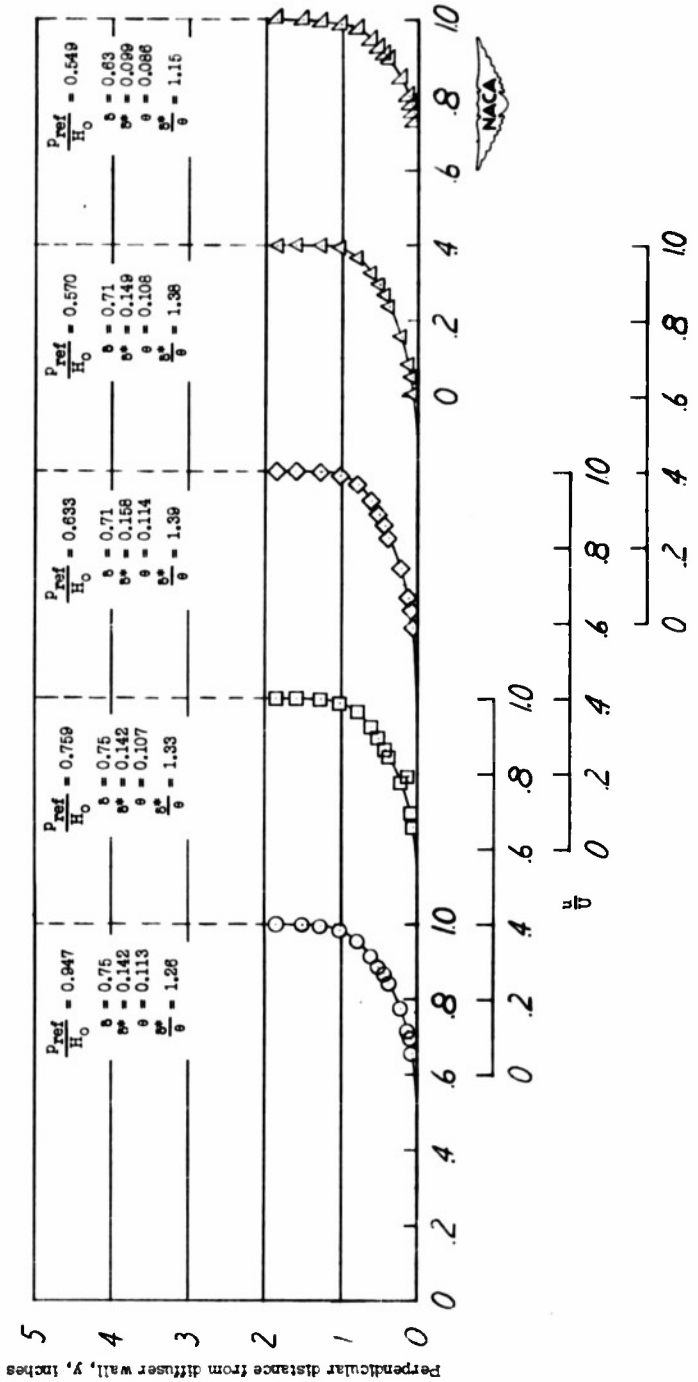

(b) Station 2.

Figure 25.- Continued.

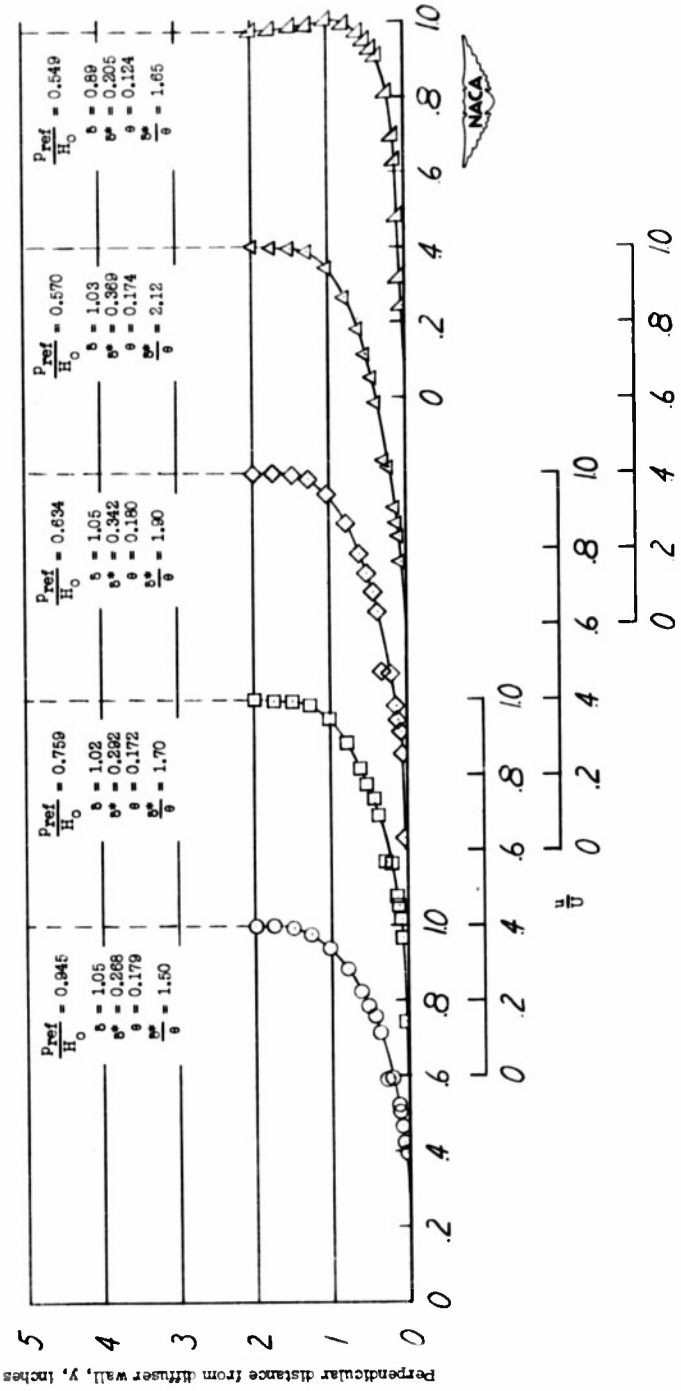

(c) Station 3.

Figure 25.- Continued.

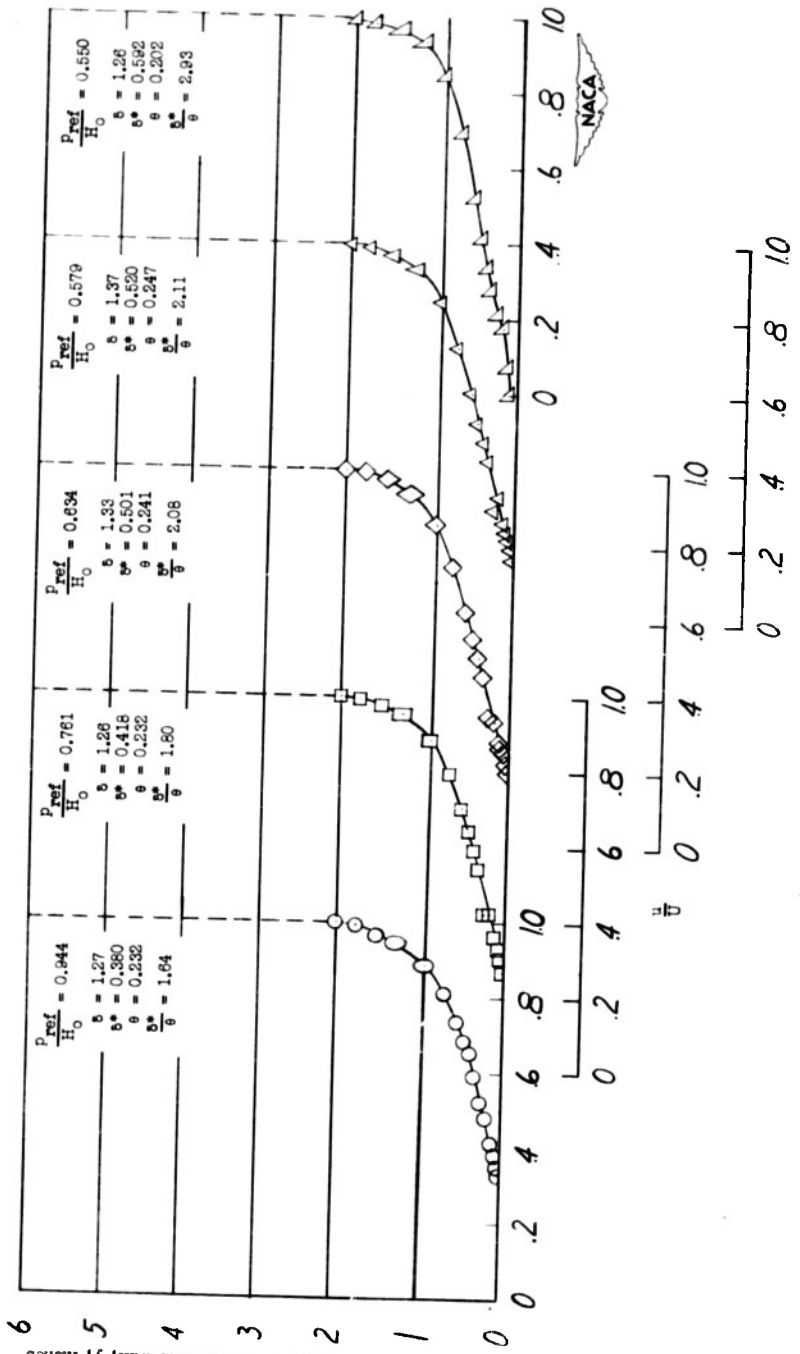

(d) Station 4.

Figure 25.- Continued.

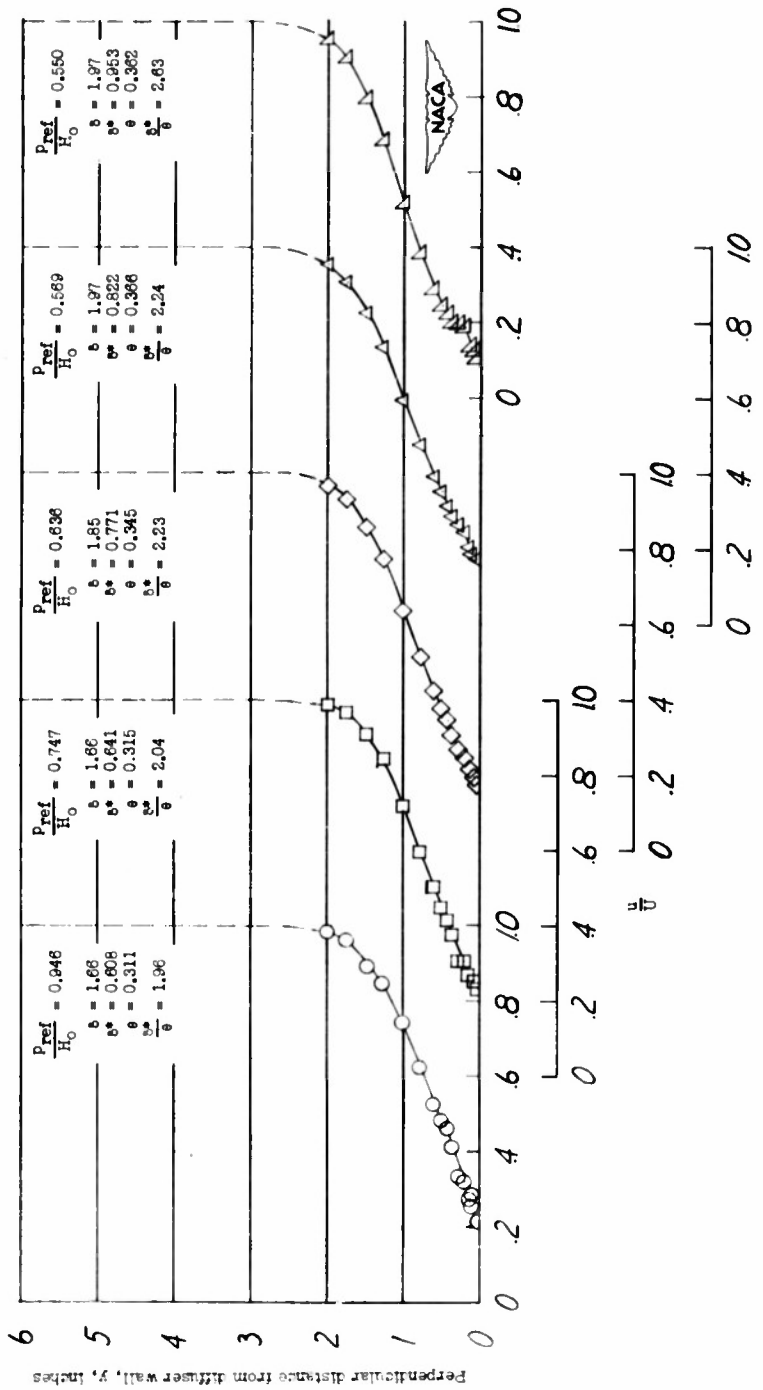

(e) Station 5.

Figure 25.- Continued.

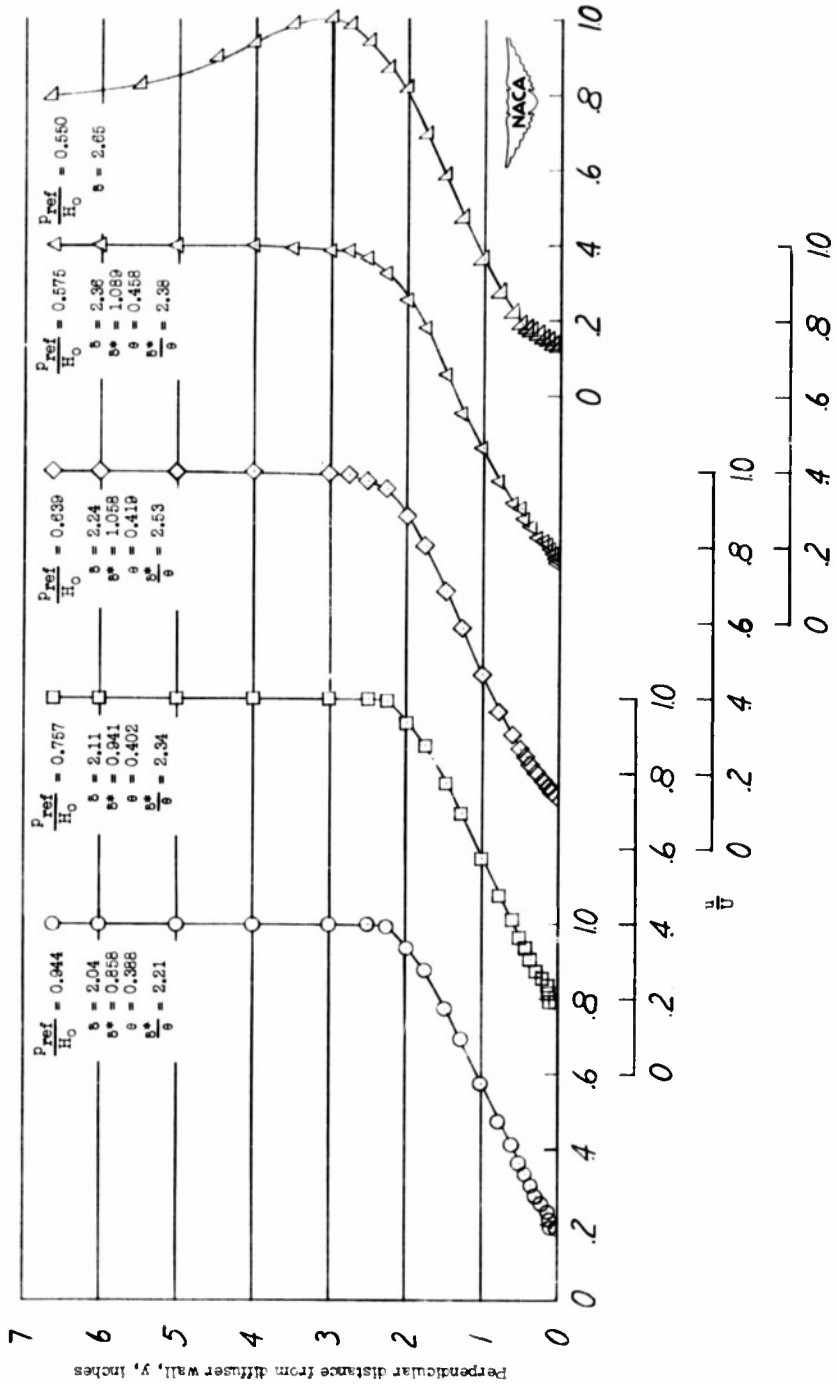

(f) Station 6.

Figure 25.- Continued.

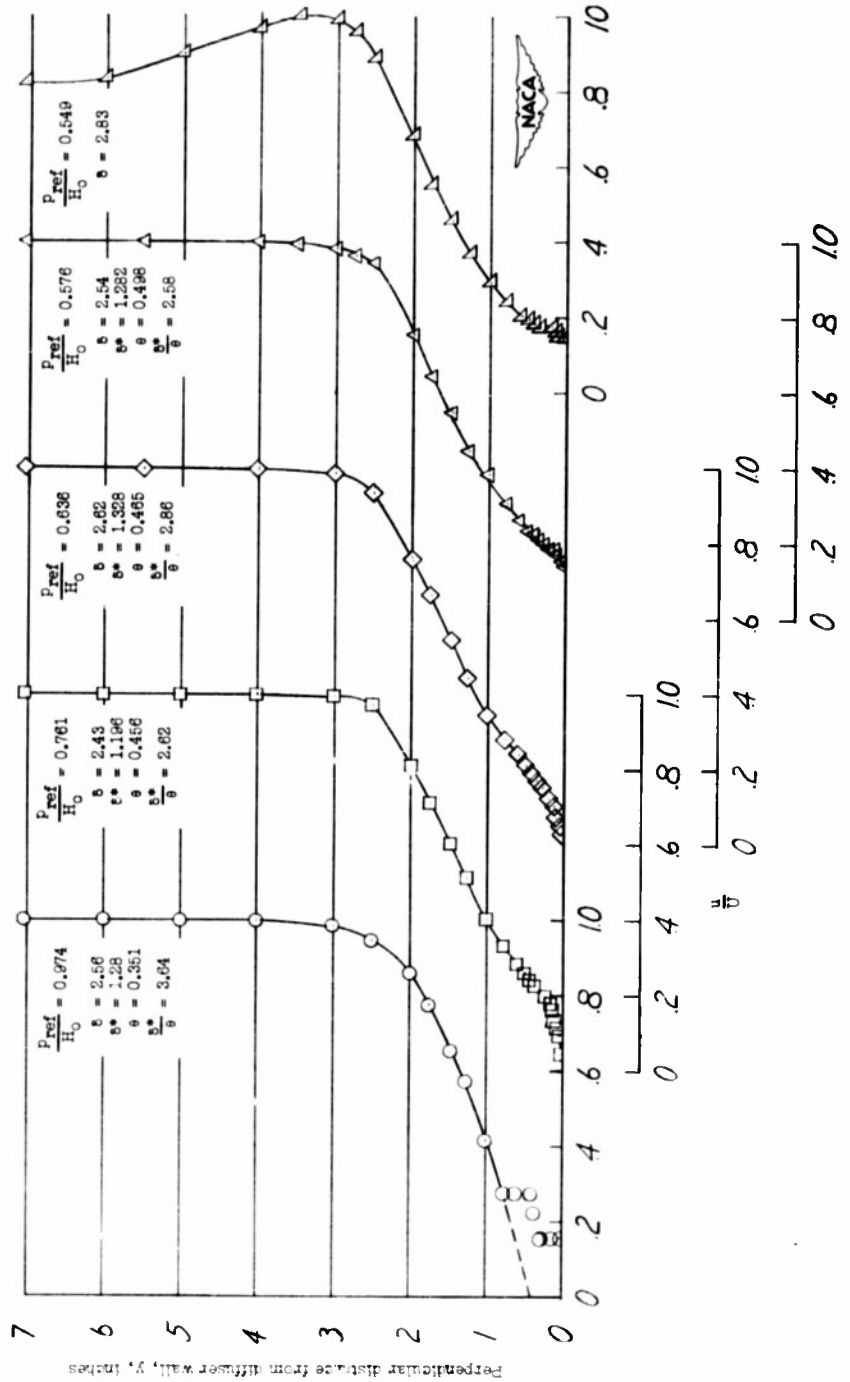

(g) Station 7.

Figure 25.- Concluded.

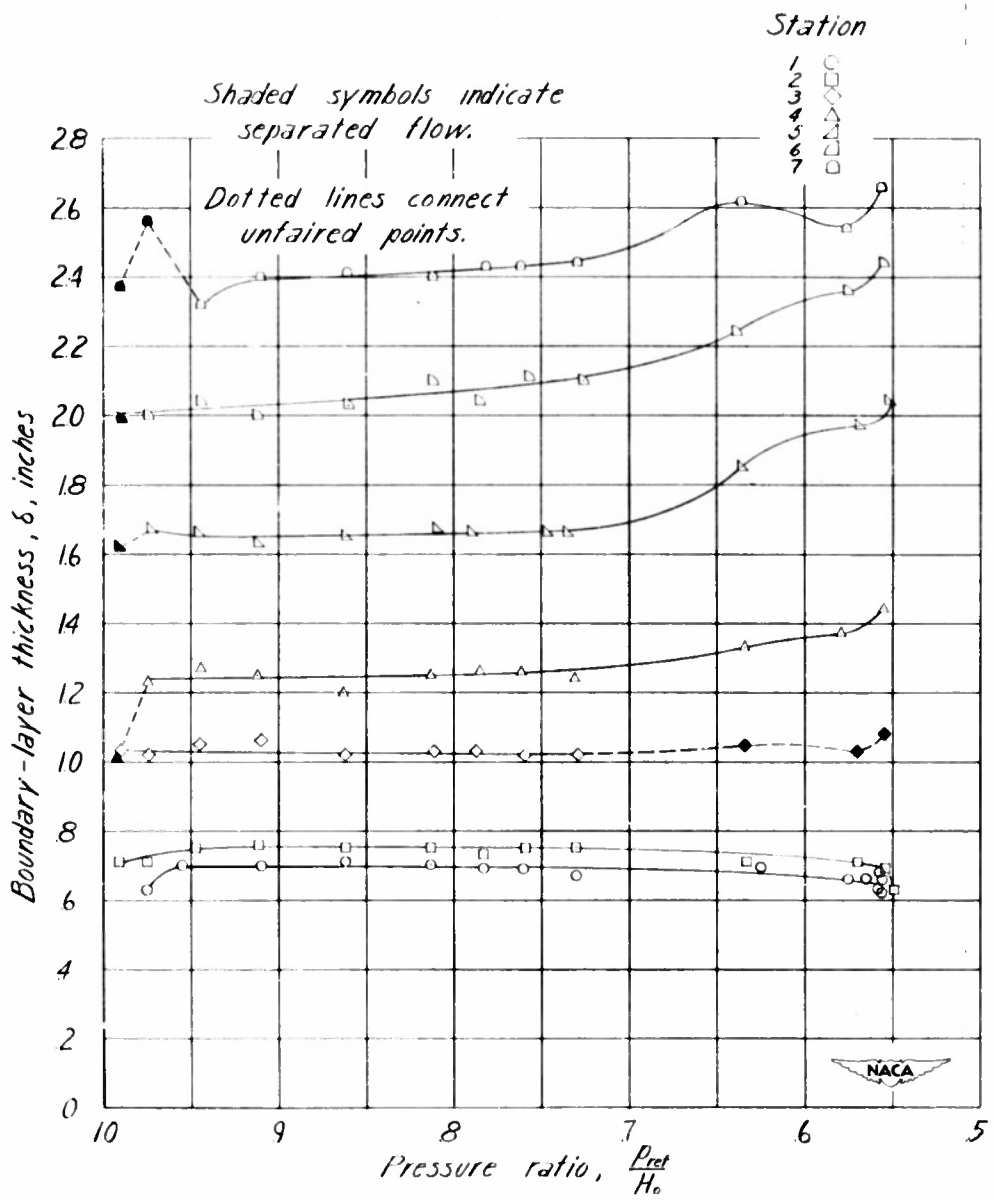

Figure 26.- Variation of boundary-layer thickness with pressure ratio - thicker inlet boundary layer.

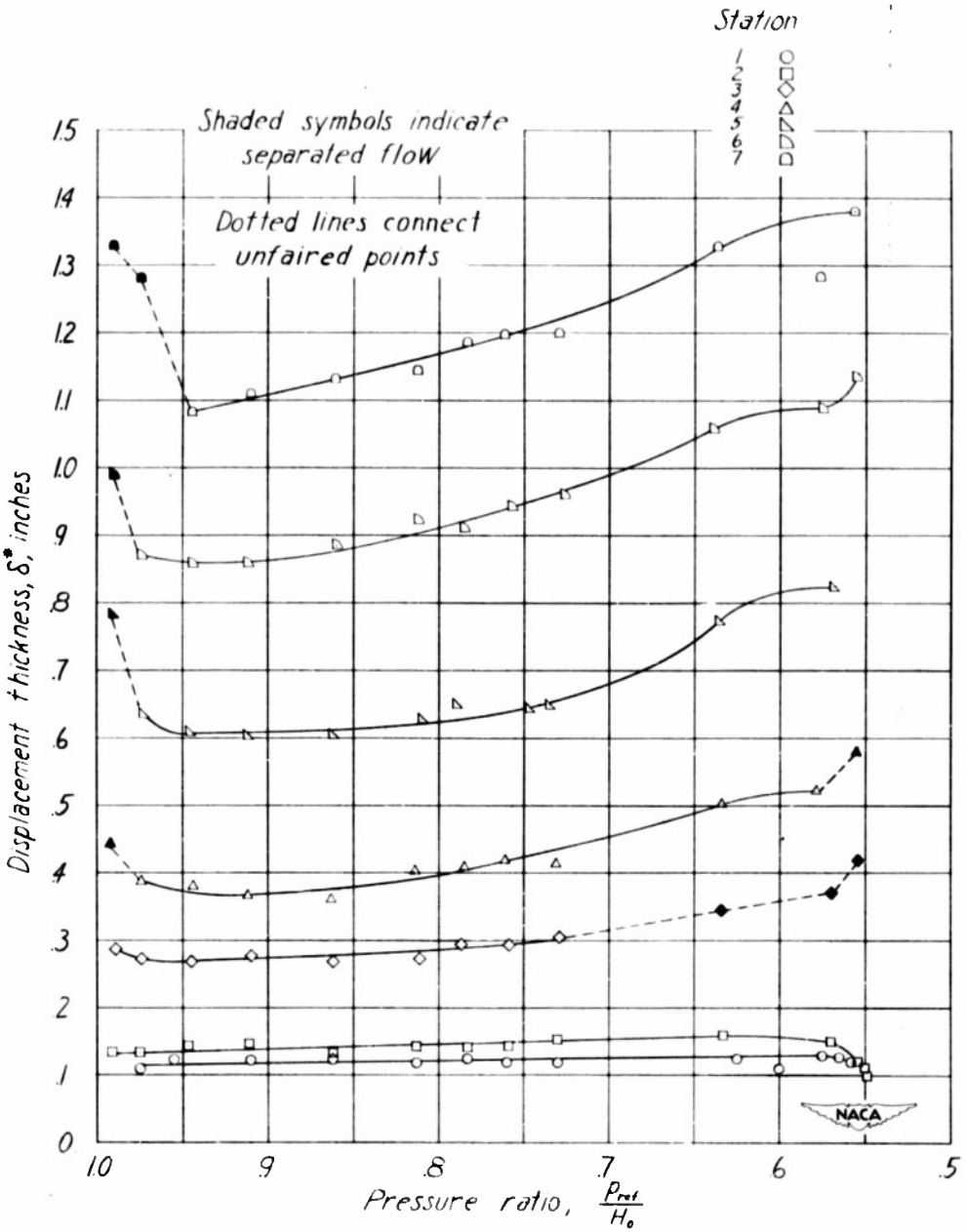

Figure 27.- Variation of displacement thickness with pressure ratio - thicker inlet boundary layer.

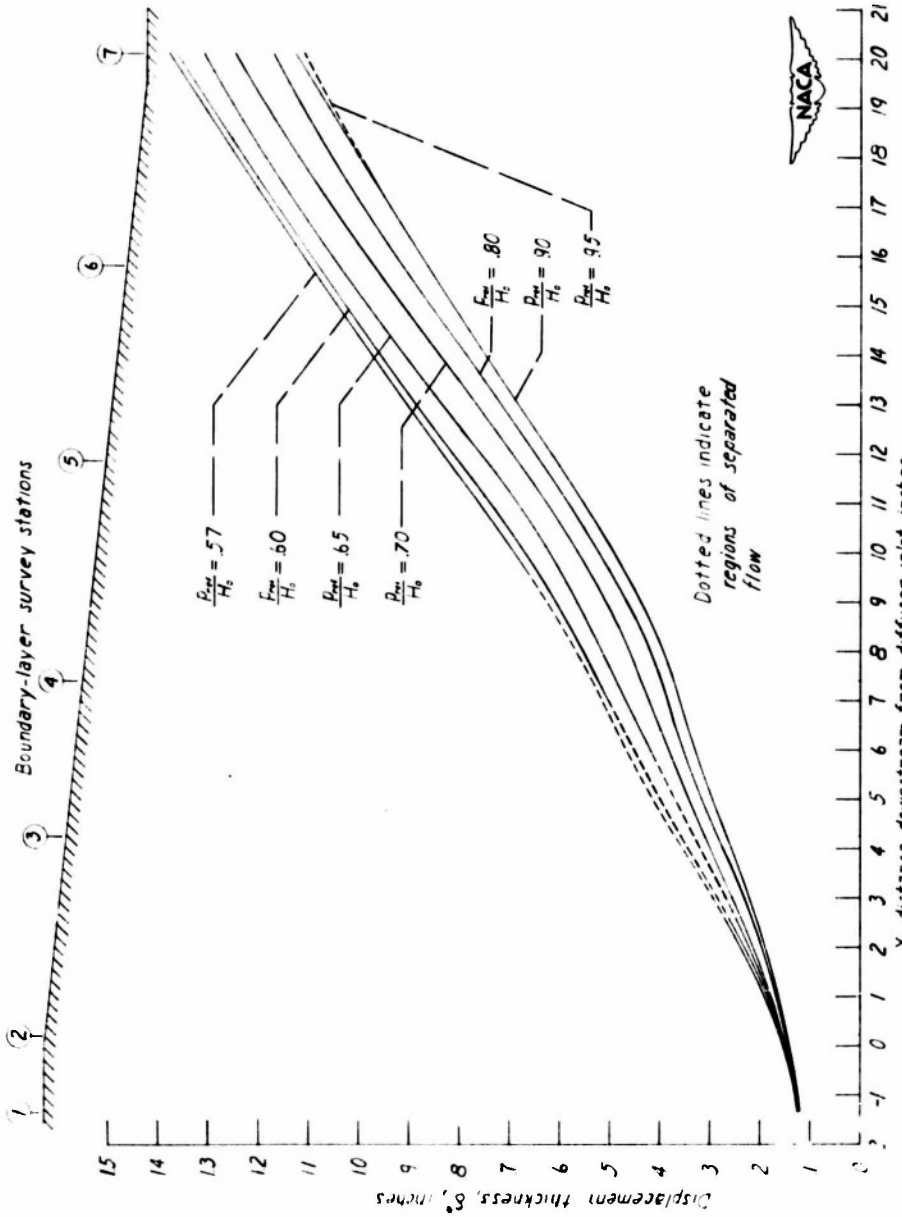

Figure 28.- Growth of displacement thickness in the thicker-inlet-boundary-layer diffuser.

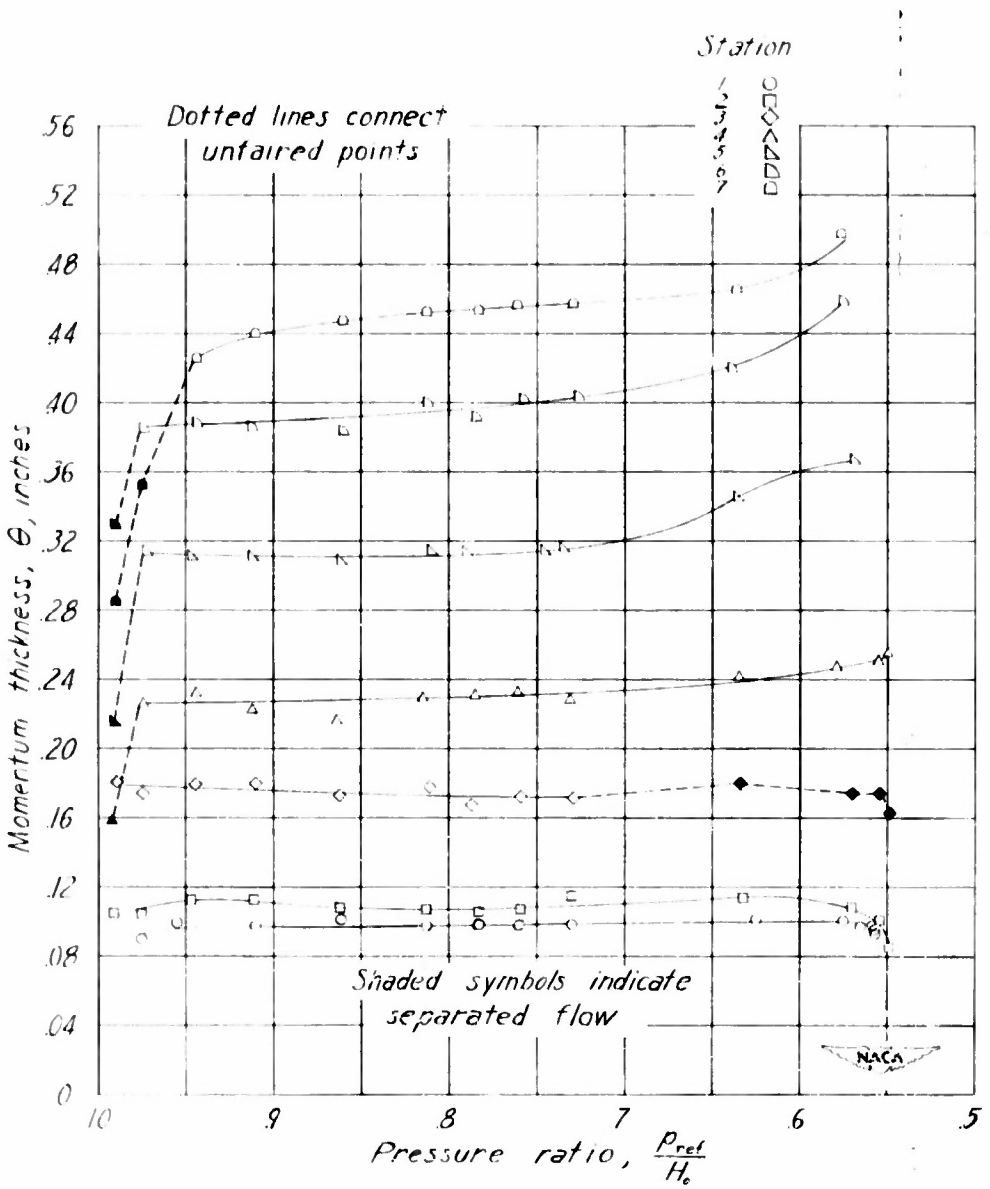

Figure 29.- Variation of momentum thickness with pressure ratio - thicker inlet boundary layer.

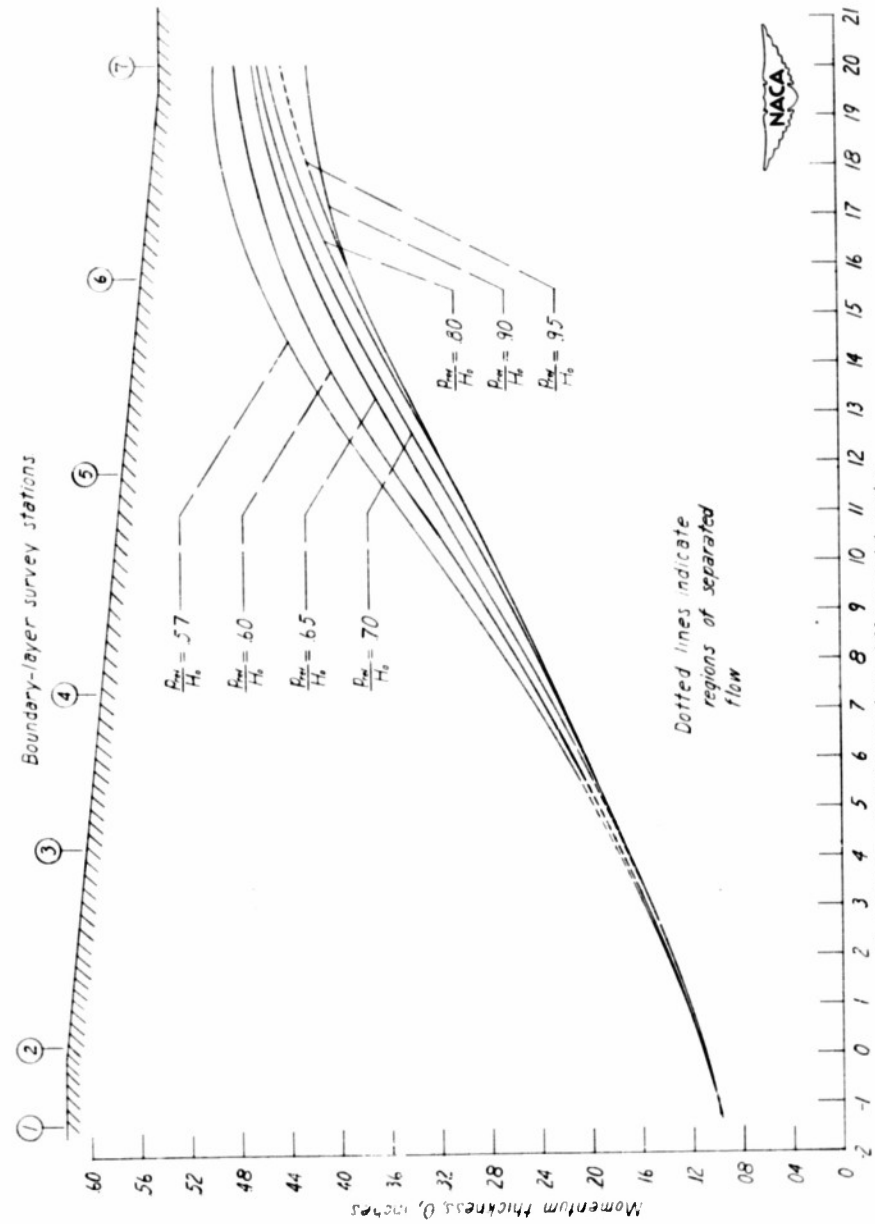

Figure 30.- Growth of momentum thickness in the thicker-inlet-boundary-layer diffuser.

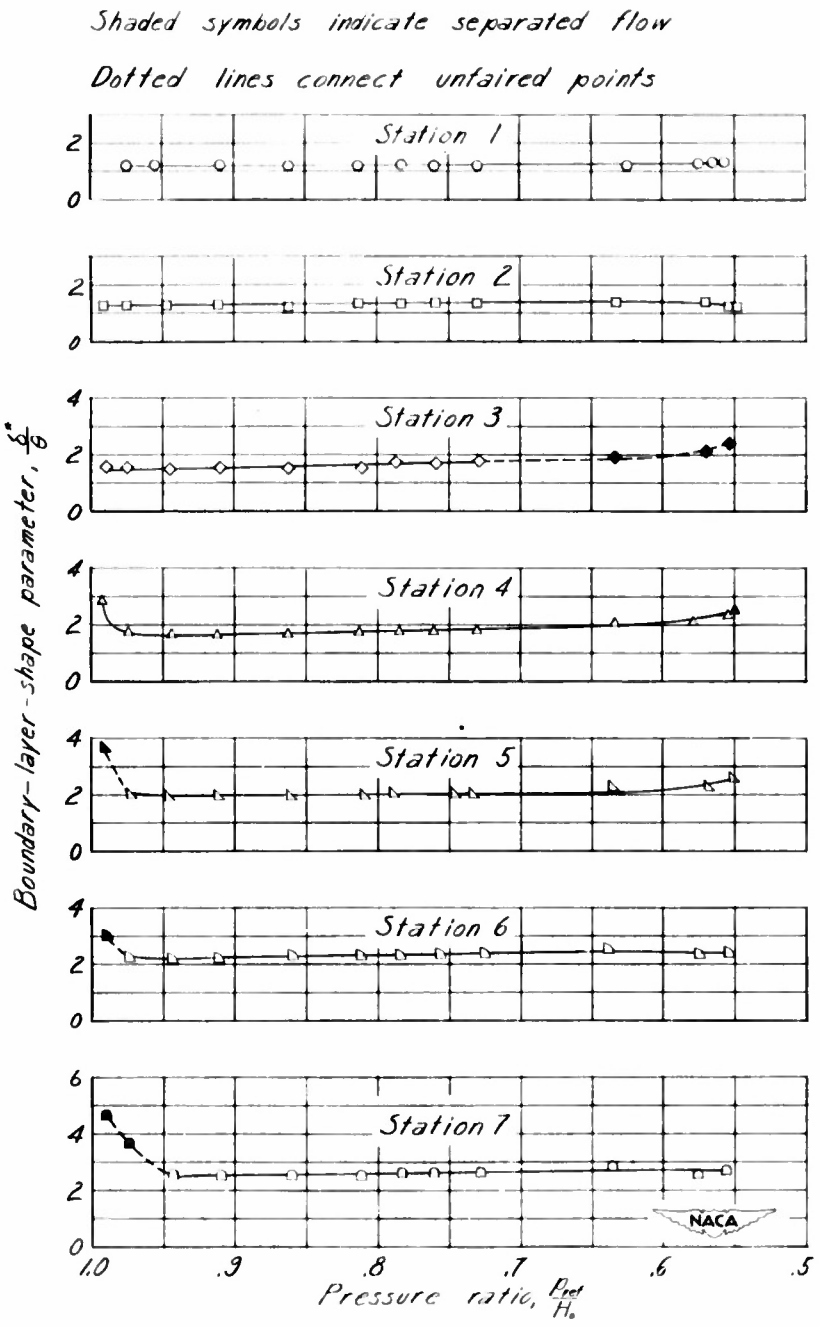

Figure 31.- Variation of boundary-layer-shape parameter with pressure ratio - thicker inlet boundary layer.

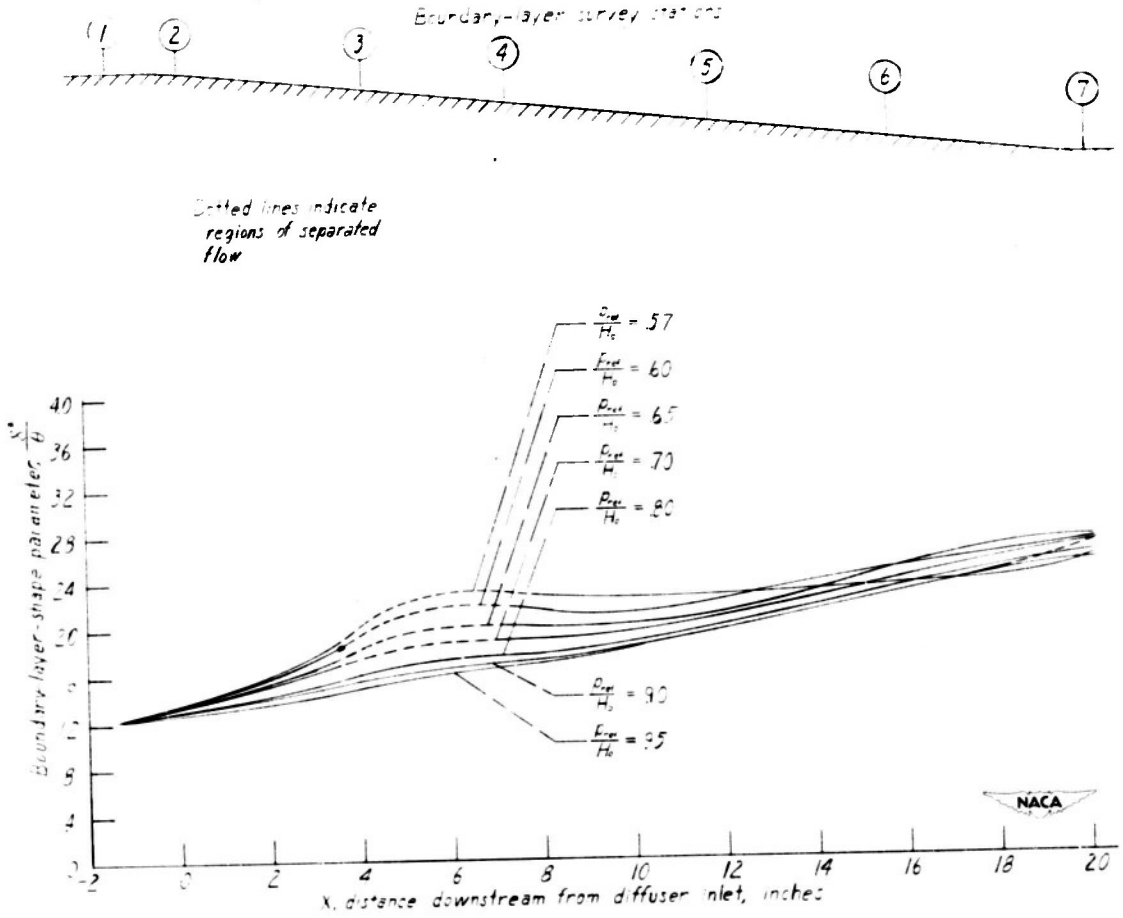

Figure 32.- Growth of boundary-layer-shape parameter in the thicker-inlet-boundary-layer diffuser.

NACA-Langley - 5-11-50 - 450

RESTRICTED

Flow, Subsonic 1.1.2.1

NACA

High-Subsonic Performance Characteristics and Boundary-Layer Investigations of a 12° 10-Inch-Inlet-Diameter Conical Diffuser.

By B. H. Little, Jr. and Stafford W. Wilbur

NACA RM L50C02a
May 1950

RESTRICTED

RESTRICTED

Flow, Turbulent 1.1.3.2

NACA

High-Subsonic Performance Characteristics and Boundary-Layer Investigations of a 12° 10-Inch-Inlet-Diameter Conical Diffuser.

By B. H. Little, Jr. and Stafford W. Wilbur

NACA RM L50C02a
May 1950

RESTRICTED

RESTRICTED

Diffusers, Subsonic 1.4.2.1.1

NACA

High-Subsonic Performance Characteristics and Boundary-Layer Investigations of a 12° 10-Inch-Inlet-Diameter Conical Diffuser.

By B. H. Little, Jr. and Stafford W. Wilbur

NACA RM L50C02a
May 1950

RESTRICTED

RESTRICTED

Boundary Layer, Internal Aerodynamics 1.4.7

NACA

High-Subsonic Performance Characteristics and Boundary-Layer Investigations of a 12° 10-Inch-Inlet-Diameter Conical Diffuser.

By B. H. Little, Jr. and Stafford W. Wilbur

NACA RM L50C02a
May 1950

RESTRICTED

RESTRICTED

Abstract

An investigation was made of the effect of inlet-boundary-layer thickness and Mach number on the performance of a 12° 10-inch-inlet-diameter conical diffuser of 2:1 area ratio. Inlet Mach number was varied from 0.2 to choking and Reynolds number (based on inlet diameter) from 1×10^6 to 3.9×10^6.

Performance coefficients, static-pressure distributions, boundary-layer profiles at seven stations in the diffuser, and boundary-layer parameters are presented.

RESTRICTED

RESTRICTED

Abstract

An investigation was made of the effect of inlet-boundary-layer thickness and Mach number on the performance of a 12° 10-inch-inlet-diameter conical diffuser of 2:1 area ratio. Inlet Mach number was varied from 0.2 to choking and Reynolds number (based on inlet diameter) from 1×10^6 to 3.9×10^6.

Performance coefficients, static-pressure distributions, boundary-layer profiles at seven stations in the diffuser, and boundary-layer parameters are presented.

RESTRICTED

RESTRICTED

Abstract

An investigation was made of the effect of inlet-boundary-layer thickness and Mach number on the performance of a 12° 10-inch-inlet-diameter conical diffuser of 2:1 area ratio. Inlet Mach number was varied from 0.2 to choking and Reynolds number (based on inlet diameter) from 1×10^6 to 3.9×10^6.

Performance coefficients, static-pressure distributions, boundary-layer profiles at seven stations in the diffuser, and boundary-layer parameters are presented.

RESTRICTED

RESTRICTED

Little, B. H., Jr., and Wilbur, Stafford W.

NACA

High-Subsonic Performance Characteristics and Boundary-Layer Investigations of a 12° 10-Inch-Inlet-Diameter Conical Diffuser.

By B. H. Little, Jr. and Stafford W. Wilbur

NACA RM L50C02a
May 1950

RESTRICTED

NACA

NACA

NACA

RESTRICTED

Abstract

An investigation was made of the effect of inlet-boundary-layer thickness and Mach number on the performance of a 12° 10-inch-inlet-diameter conical diffuser of 2:1 area ratio. Inlet Mach number was varied from 0.2 to choking and Reynolds number (based on inlet diameter) from 1×10^6 to 3.9×10^6.

Performance coefficients, static-pressure distributions, boundary-layer profiles at seven stations in the diffuser, and boundary-layer parameters are presented.

RESTRICTED

RESTRICTED

Abstract

An investigation was made of the effect of inlet-boundary-layer thickness and Mach number on the performance of a 12° 10-inch-inlet-diameter conical diffuser of 2:1 area ratio. Inlet Mach number was varied from 0.2 to choking and Reynolds number (based on inlet diameter) from 1×10^6 to 3.9×10^6.

Performance coefficients, static-pressure distributions, boundary-layer profiles at seven stations in the diffuser, and boundary-layer parameters are presented.

RESTRICTED

RESTRICTED

Abstract

An investigation was made of the effect of inlet-boundary-layer thickness and Mach number on the performance of a 12° 10-inch-inlet-diameter conical diffuser of 2:1 area ratio. Inlet Mach number was varied from 0.2 to choking and Reynolds number (based on inlet diameter) from 1×10^6 to 3.9×10^6.

Performance coefficients, static-pressure distributions, boundary-layer profiles at seven stations in the diffuser, and boundary-layer parameters are presented.

RESTRICTED

CADO CONTROL NO.: (N.A.)

US CLASSIFICATION: [redacted]

ATI NO.: 75 592

QA NO.: NACA RM L50C02A

TITLE: High-Subsonic Performance Characteristics and Boundary-Layer Investigations of a 12° 10-Inch-Inlet-Diameter Conical Diffuser (Research Memorandum). 11 May 1950. 62 pp. 2 refs

U

AUTHOR(S): Little, B.H.Jr.; Wilbur, Stafford, W.

5-2

ORIGINATING AGENCY: National Advisory Committee for Aeronautics, Langley Aeronautical Lab., Langley Air Force Base, Va.

FOREIGN TITLES: (N.A.)

27 2

PUBLISHED BY: (Same)

PUBLISHING NO.: (Same)

TRANSLATED BY: (N.A.)

TRANSLATION NO.: (N.A.)

PREVIOUSLY CATALOGED AS: (N.A.)

AIR FORCE-WPAFB-12 MAY 50 1000N

CADO FORM NO. 8C — LIBRARY CARD

Power Plants, Jet & Turbine (5)
Induction System (2)

Classification cancelled
or ~~changed to~~ Unclassified
NACA Res Abstracts No 46, dtd 31 July '53
AUTH:
By Dorothy S Fischer OSA
Signature and Grade

Date 5 Oct '53

CADO CONTROL NO.:	US CLASSIFICATION:	ATI NO.:	NACA RM
(N.A.)	Restr.	75 592	L50C02A

TITLE: High-Subsonic Performance Characteristics and Boundary-Layer Investigations of a 12° 10-Inch-Inlet-Diameter Conical Diffuser (Research Memorandum), 11 May 1950. 62 pp.

AUTHOR(S):
Little, B.H.Jr.; Wilbur, Stafford, W.

ORIGINATING AGENCY: National Advisory Committee for Aeronautics, Langley Aeronautical Lab., Langley Air Force Base, Va.

FOREIGN TITLES:
(N.A.)

PUBLISHED BY:	PUBLISHING NO.:
(Same)	(Same)

TRANSLATED BY:	TRANSLATION NO.:
(N.A.)	(N.A.)

PREVIOUSLY CATALOGED AS:
(N.A.)

AIR FORCE-WPAFB-12 MAY 50 1000

CADO FORM NO. 5C — LIBRARY CARD